

**Simulated Signal and Noise Profiles  
in Distribution Line Carrier Networks**

by

**Daniel C. Borowski**

**Center for Communications and Signal Processing  
Department of Electrical and Computer Engineering  
North Carolina State University**

**January 1986**

**CCSP-TR-86/1**

## ABSTRACT

Borowski, Daniel C. Simulated Signal and Noise Profiles in Distribution Line Carrier Networks (under the direction of Dr. J. B. O'Neal, Jr.)

The purpose of this study was to simulate and measure Distribution Line Carrier signal propagation in a controlled single-phase overhead power distribution network. The network conforms to the simplest model of a distribution line network, possessing a tree topology with one branch. The empirical data is compared to that predicted using the equations of transverse electromagnetic (TEM) mode of signal propagation; the predicted values are found to be in error in excess of 60%. The error is due to uncertainty in the electrical lengths of the lines. A sensitivity analysis of the network response to variations in the line electrical lengths reveals that, for this particular network configuration, reasonably accurate predicted values cannot be achieved given typical field measurements of line lengths.

A simple demonstration of the reciprocity relation between three network pairs of "ports" is conducted. Because of this relation, the analysis of the network is simplified by calculating the transfer impedance between the source and other points in the network.

A practical means of artificially loading complex networks to improve the signal profile is investigated. While "weak spots" in the signal profile are ameliorated by this approach, the performance of the system is degraded by a reduction in the average transimpedance between the source and other points in the network.

Noise profiles are simulated by exciting the network from three different remote ports, first individually and then simultaneously by phase-locked sources. In both cases, the signal-to-noise ratio is found to be dependent upon location in the network.

The author wishes to thank Dr. J. B. O'Neal and Fathi Amoura of North Carolina State University; Lou Gale, Kay Clinard and the other employees of the Distribution Research & Engineering Unit of Carolina Power & Light; and Ken Shuey of Westinghouse Corp. for their support in this research.

Special thanks also to Professor W. T. Easter of North Carolina State University.

The author also wishes to thank his wife for her patience, understanding and encouragement throughout this endeavor.

## TABLE OF CONTENTS

	Page
1. INTRODUCTION	1
2. CALCULATION OF RESPONSE IN THE MODEL DISTRIBUTION LINE NETWORK	3
2.1 Equations for TEM mode of signal propagation	3
2.2 Extension of equations to branched networks	7
2.3 Effects of line termination and source impedance variations on the network response	11
2.4 Computer simulation of DLC signal in the network model	16
3. TEST NETWORK DESCRIPTION	19
3.1 Factor affecting the test network selection	19
4. FIELD TESTS	23
4.1 Demonstration of symmetry of transfer impedance	23
4.2 Measurements of signal propagation in the test network	32
4.3 Artificial loading to improve network response	49
4.4 Simulation of noise profile	56
5. CONCLUSIONS	68
6. LIST OF REFERENCES	70

## INTRODUCTION

Distribution Line Carrier (DLC) communication systems employ the utilities' own network of power distribution lines as a medium for the transmission of information. The applications of these systems include such functions as remote meter reading, load control, capacitor bank dispatch, outage location, etc. The advantages of such systems from the utility standpoint are numerous, including direct ownership and control of the network [CLI].

In its most basic form, a DLC system superimposes a high frequency modulated signal onto the power distribution lines. This signal usually originates from a central unit typically located at the distribution substation, although bidirectional systems employing transmitters at many remote locations are becoming commonplace. These signals suffer attenuation as they propagate along the network of distribution lines, traversing complex paths usually exhibiting multiple levels of branching, and through electrical equipment designed for the efficient distribution of low frequency power. In addition, the length of the lines in most networks is a significant fraction of an electrical wavelength at typical DLC frequencies. Hence, transmission line effects become prominent, and such phenomenon as standing waves giving rise to signal nulls may create problems in some DLC networks. Furthermore, the level of noise on these systems poses concern [ONE]. Clearly, there are many factors contributing to the uncertainty of the performance of these systems.

There has been considerable research done to characterize the elements that make up DLC systems and develop models of these elements des-

cribing their effects on DLC signals [HEM, GEN, SHU]. This research has contributed significantly toward an understanding of how a DLC system may be expected to perform.

In this paper, the results of the research above has been applied in an attempt to predict the performance of a typical DLC system. The ability to make such predictions is vital in designing and evaluating these systems with confidence. Empirical data gathered from field tests on a simulated network is compared to predicted values, to assess the accuracy achievable in making such predictions. Finally, studies are conducted on the behavior of noise injected into the test network.

## 2. CALCULATION OF RESPONSE IN THE MODEL DISTRIBUTION LINE NETWORK

### 2.1 Equations for TEM mode of signal propagation

It has been observed [HEM] that energy signals at typical DLC frequencies propagate along distribution lines in the transverse electromagnetic (TEM), or transmission line, mode. The parameters that describe this mode of propagation (e.g., line characteristic impedance, propagation constant) are functions of the media and geometry of the distribution line structure. The derivation of the modal parameters will not be discussed here. It is the intent of this section to develop the equations which characterize the propagation of DLC signals in typical distribution line networks.

The propagation of signals along a single transmission line section is described by the solutions to the TEM wave equations, which are [PAR]

$$V(z) = V_+ \exp(-c*z) + V_- \exp(c*z) \quad (2.1.1)$$

$$I(z) = (V_+ \exp(-c*z) - V_- \exp(c*z))/Z_0 \quad (2.1.2)$$

where:

$c$  is the propagation constant

$Z_0$  is the line characteristic impedance

$z$  is the position on the line, measured from the source

$V_+$  and  $V_-$  are arbitrary constants, which can be evaluated at the boundary conditions of the line. The boundary conditions must be satisfied at points of discontinuity, that is, where loads or sources are connected, at branch points, etc.

Consider the section of line in Figure 2.1.1, connecting a practical source to a load. Arbitrarily choosing the source end of the line as the origin ( $z=0$ ) we find

$$V_0 = V^+ + V^- \quad (2.1.3)$$

$$I_0 = (V^+ - V^-)/Z_0 \quad (2.1.4)$$

Solving for the arbitrary constants, we find

$$V^+ = (V_0 + I_0 Z_0)/2 \quad (2.1.5)$$

$$V^- = (V_0 - I_0 Z_0)/2 \quad (2.1.6)$$

$V_0$  and  $I_0$  can be found if the input impedance of the network is known.

In this case,

$$I_0 = V_S / (Z_S + Z_{in}) \quad (2.1.7)$$

$$V_0 = V_S * (Z_{in} / (Z_{in} + Z_S)) \quad (2.1.8)$$

The impedance at any point along a line is simply the ratio of line voltage and current. Hence,

$$Z(z) = Z_0 * \frac{V^+ \exp(-c*z) + V^- \exp(c*z)}{V^+ \exp(-c*z) - V^- \exp(c*z)} \quad (2.1.9)$$

In this case, it is convenient to choose the position of the load as the origin ( $z=0$ ), with  $z$  decreasing and hence negative toward the source. Dividing numerator and denominator of (2.1.9) by  $V^+ \exp(-c*z)$ , we get

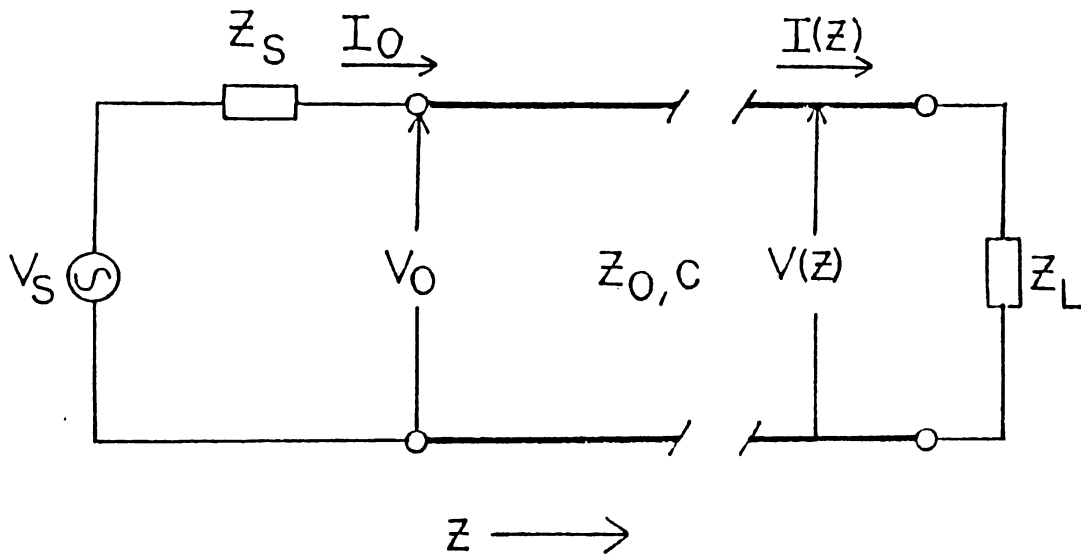


FIGURE 2.1.1 Transmission line connecting a practical source to a load.

$$Z(z) = Z_0 \frac{1 + (V^-/V^+) \exp(2\gamma z)}{1 - (V^-/V^+) \exp(2\gamma z)} \quad (2.1.10)$$

$$= Z_0 \frac{1 + p \exp(2\gamma z)}{1 - p \exp(2\gamma z)} \quad (2.1.11)$$

where  $p = V^-/V^+$  is the reflection coefficient of the load.

The reflection coefficient, which in general is complex, can be calculated as

$$p = \frac{Z_1 - Z_0}{Z_1 + Z_0} \quad (2.1.12)$$

where  $Z_1$  is the impedance of the load.

Therefore, knowing the load impedance and its position on the line, as well as the modal parameters of the line, the input impedance of the line can be calculated. Then, from a knowledge of the input impedance, the arbitrary constants  $V^+$  and  $V^-$  that satisfy the boundary conditions at the source end can be evaluated, and the wave equations completely described.

## 2.2 Extension of equations to branched networks

In practical distribution networks, branching (transmission line junctions) is pervasive. Therefore, to be able to model and predict signal strength in actual networks, an analysis of the effect of branching on signal propagation must be made.

Consider the simple network depicted in Figure 2.2.1, consisting of a transmission line connecting a source to a branch, or junction of two transmission lines, each of which, in turn, is connected to arbitrary passive loads. As noted in the previous section, the branch forms a discontinuity, at which the boundary conditions must be satisfied.

Using equation (2.1.11) from the previous section, the input impedance of each branch section can be calculated, if the length of the branch section, value of the load, and modal parameters of the line section is known. Thus, the branch sections can be replaced by equivalent impedances, the parallel combination of which forms the load impedance on the section feeding the branch. The arbitrary constants, and hence the complete wave equations of the feeder section can then be evaluated.

Note this procedure can be extended to branches of  $n$  sections,  $n$  being any positive integer, or to branch sections feeding other branched sections. In all cases, the network is reduced such that the network driving point (input) impedance is known.

What remains to be solved is the arbitrary constants  $V^+$  and  $V^-$  of the branch sections. These constants can be solved using equations (2.1.5)

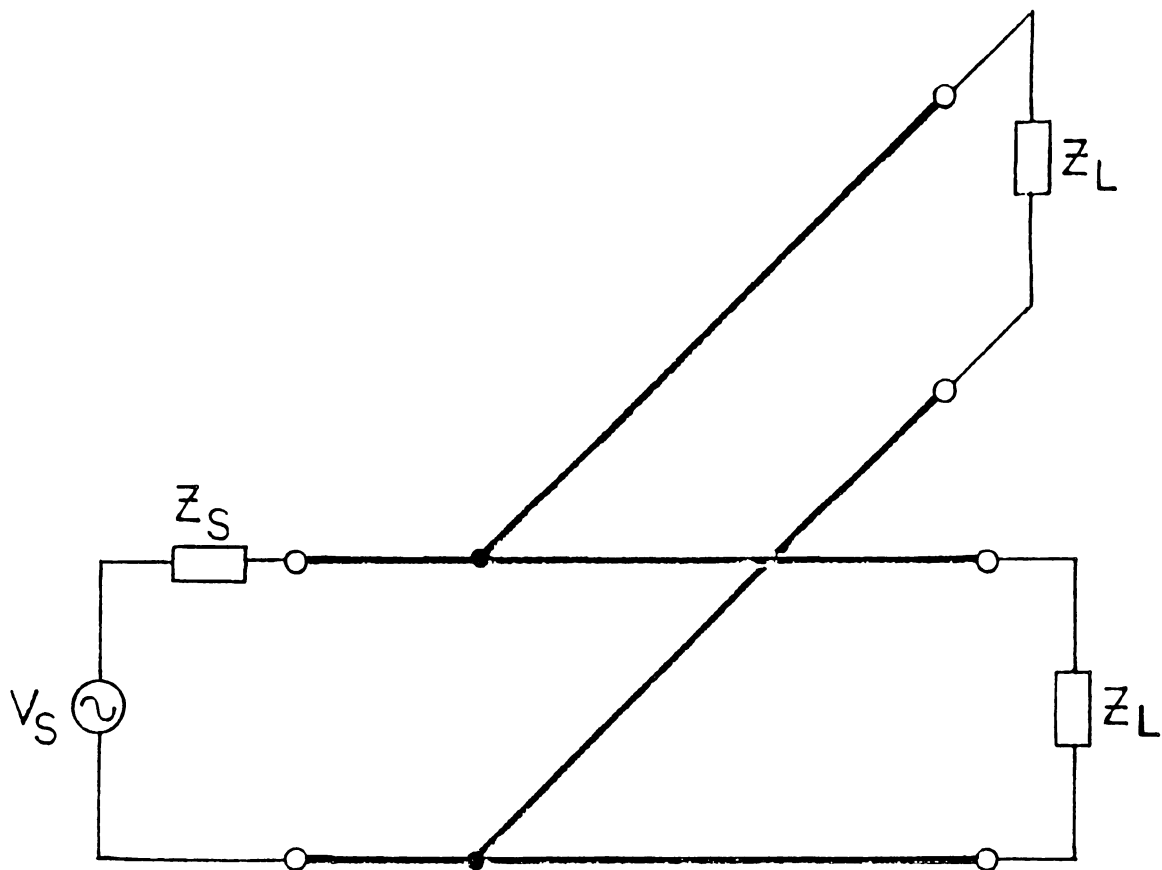


FIGURE 2.2.1 Source driving a network consisting of a line feeding a branch of two line sections.

and (2.1.6) if the voltage  $V_0$  at the source end of the branch section, and the current  $I_0$  entering each branch are known. Since the line voltage is continuous in the region of the branch [PAR],  $V_0$  for each branch can be found by solving for the line voltage at the branch end of the line feeding the branch, using equation (2.1.1). In addition, the current  $I(z)$  (from equation (2.1.2)) in the line section feeding the branch will be divided between the two branch sections in proportion to the input admittance of each branch section. Thus, the arbitrary constants  $V^+$  and  $V^-$  for each branch section can be evaluated, and hence the line voltage and current along each of the branch sections [CRE].

As noted earlier, this procedure can be extended to branches of any number of sections, or to branch sections feeding other branched sections. Such networks are described as having a "tree" topology, and it is this network topology which is typical of most distribution line networks. The network of a single line feeding a branch of two sections is the simplest type of tree network, and as such forms a model of the typical distribution line network. Most real distribution line networks are thus extensions of this simple model.

Note that using the analysis outline above, the line voltage  $V(z)$  and line current  $I(z)$  can be determined anywhere within the network. In practice, however, the magnitude of the DLC signal which is present at the remote receivers is dependent only upon the line voltage. This is because most remote receivers are coupled to the secondaries of the distribution transformers. The primaries of the distribution transformers are connected between the phase and neutral conductors, and as such are potential transformers. In addition, the input impedance of

the primary circuit of the distribution transformer is very high at typical DLC frequencies [SHU], and therefore the distribution transformers can be ignored in the prediction process. For these reasons, the line voltage  $V(z)$  is the parameters of interest, and will be called the "network response" to a source excitation throughout this paper.

This model and the mathematical description of a signal propagating throughout it, have been verified by field tests. The results of these field tests will be discussed in a later section.

### 2.3 Effect of line termination and source impedance variations on the network response

It is instructive to analyze the effects of line termination and source impedance variations on the network response. As discussed in Section 2.1, the loads and sources connected to the network represent points of discontinuity, and form the boundary conditions at which the arbitrary constants  $V^+$  and  $V^-$  describing the wave equations may be evaluated. To examine the effects the load and source impedance have on the response, consider the simple case of a single section of a single transmission line connecting a source to a load, as depicted in Figure (2.1.1). As explained in Section 2.2, this simple case can be extended to the case of a more complicated network in a straight forward manner. Since nearly all distribution lines are terminated into an open-circuit (or an impedance high enough to be considered essentially an open circuit), this special case is considered here.

From equation (2.1.12), the reflection coefficient of an open-circuit ( $Z_l \rightarrow \text{infinity}$ ) is

$$\text{po.c.} = +1/0 \quad (2.3.1)$$

Thus, any voltage wave encountering an open-circuit is completely reflected, and the reflected wave is in phase with the forward wave. Because of this relation between the forward and reflected waves, a voltage relative maxima always occurs at an open-circuit (when the line losses are low). Furthermore, rewriting equation (2.1.1) by choosing

the load end of the line as the origin ( $z=0$ , decreasing and negative away from the load) and substituting the definition of the reflection coefficient for the load yields

$$V(z) = V_+ \exp(-c*z) * (1 + p*\exp(2*c*z)) \quad (2.3.2)$$

The magnitude of the response is

$$|V(z)| = |V_+| * |1 + p*\exp(2*c*z)| \quad (2.3.3)$$

This analysis points out that the reflection coefficient of the load solely determines the position of the line voltage maxima and minima (generating the "standing wave pattern").

Note since there are two arbitrary constants in equation (2.1.1), the complete solution is determined by both boundary conditions, at the load and at the source. The boundary condition at the source is evaluated using equations (2.1.3) to (2.1.8).

Any monochromatic source can be modelled as a practical Norton source consisting of an ideal current source in parallel with a source admittance. What is of interest here is an assessment of the effect of variations of these elements of the source on the network response. As discussed above, the position of the response relative extrema is determined solely by the load characteristics. Clearly then, no changes at the source end of the line can alter the location of these points. It seems intuitive, however, that some parameter of the response must change as the source is changed.

Consider the source magnitude first. Since the network is linear (see Section 4.1), changing the source magnitude will result in an equal change in the network response. (This can also be seen by examining equations (2.1.8) and (2.1.3)).

Now consider the source impedance. Obviously, changing the source impedance will result in a change in the current entering the network, given a fixed source magnitude and network configuration (see equation (2.1.7)). Likewise, the arbitrary constants  $V^+$  and  $V^-$  will both change in proportion to the change in input current. Hence, the network response will also change proportionately. Therefore, the ratio of network response to input current remains constant. This ratio is referred to as the network transfer impedance, or transimpedance.

In summary, variations of the source parameters change only the magnitude of the response. However, the ratio of the network response to a given network excitation is determined solely by the constants of the network, independent of the source [VAN].

A DLC network can be viewed as a multiport network, where the "ports" in this model correspond to points on the network lines at which communication equipment is connected. Depending on the choice of excitation and response, an  $n \times n$  matrix can be generated describing the relation between each  $n^2$  possible pairs of ports. Such relations are termed "network functions". One choice of network function is the open-circuit, or Z parameter. The elements of this matrix are computed as

$$Z_{ij} = V_i / I_j \Big|_{I_k=0 \text{ for } k=j} \quad (2.3.4)$$

where  $V_i$  is the open-circuit voltage at port  $i$ , and  $I_j$  is the current entering port  $j$ .

Notice the number of elements in the matrix grows as the square of the number of ports. This would result in a large number of calculations for even a network with relatively few ports. Fortunately, however, DLC network architecture is designed such that communication exists only between a single master, or "host", port (at the substation) and all the remote, or slave, units. The  $z$ -parameters of interest, then, are those relating the response at all  $n-1$  remote ports to an excitation at the host port. In systems employing two-way communication, the  $z$ -parameters relating the network response at the host port to excitations at each of the remote ports is also required. Thus,  $2*(n-1)$  elements must be calculated to predict the performance of the system.

It should be pointed out that there are many choices of network functions, each determined solely by the characteristics of the network. Thus, the source parameters are "normalized out". The choice of calculating the  $z$ -parameters was made for the following reasons:

- i) The input impedance of the primary circuit of the distribution transformer is high enough to be considered an open-circuit (i.e. it presents negligible loading of the line). This has been discussed in Section 2.2. Therefore, the network response is in effect the open-circuit voltage at the distribution transformer location. Therefore, knowing only the input current at the host port and the  $z$ -parameter to each remote port, the signal at the receivers can be predicted.

ii) DLC networks are reciprocal (see Section (4.1)). For reciprocal networks, the open-circuit transimpedance between port pairs is the same with the excitation at either port. Thus, the transimpedance need only be calculated for one direction of communication, while such symmetry does not exist for most other network functions (voltage transfer ratio, etc). This is beneficial when bi-directional systems are considered (e.g. the network is sourced from either the central or a remote port), since only  $(n-1)$  parameters need be considered.

## 2.4 Computer simulation of DLC signal in the network model

Reviewing equations (2.1.1) through (2.1.12), it can be seen that the calculation of signal strength in even a very simple network, while a straight forward procedure, involves the use of somewhat complicated equations. Most of the arguments in the equations are complex. In addition, the calculations involved are repetitious. Therefore, it seems practical to code the equations use in such calculations in software.

A program to execute the calculations presented in the beginning of this section was written in FORTRAN. Variable quantities in the program include the branch section load admittances, line modal parameters, and line lengths. For calculating the network response, the model network is assumed to be excited by an ideal current source, the magnitude of which is also variable. Calculation of the network transimpedance can also be specified. In this case, a unit input current is used. The program then calculates the arbitrary constants, and thus the complete wave equation for each line section. The desired output parameter can then be calculated at any point on the network; the points at which such calculations are to be made are stored in a datafile, which is read by the program.

A sample output of the program, for a fictitious network, is plotted and presented in Figure 2.4.1. The independent variable (domain) is the distance, along the network, from the source. In general, this distance is not equal to the radial distance from the source, except in those networks having line sections extending away from the source strictly along a radial line. At various points along the network, the network response (voltage from phase conductor to neutral conductor) is calcu-

## NETWORK RESPONSE

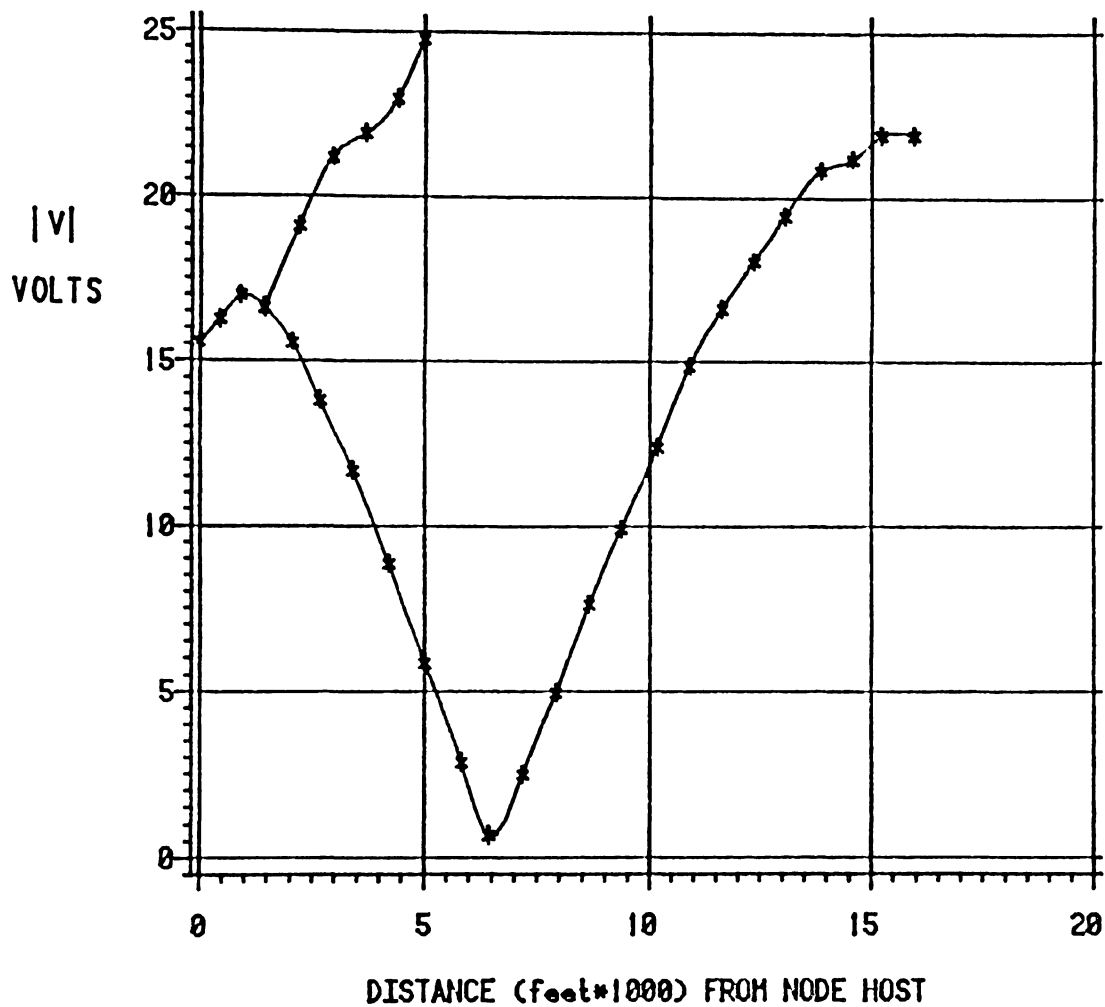


FIGURE 2.4.1 Sample Output of DLC Network Analysis Program

lated and plotted (as indicated by an asterisk). The points plotted are connected by a line during the plot procedure; the line is smoothed using a spline function.

From this example it can be seen that the network response is not everywhere a single-valued function of distance from the source. At positions where the response is double-valued, branching has occurred and the response is plotted for each section. In general, the response is not the same on each branch section for equal distances from the source.

### 3. TEST NETWORK DESCRIPTION

This section presents the test procedures used in making field measurements on actual distribution line networks. The purpose of these tests is to gather data which either supports or disproves the theory presented in the previous sections. In addition, the accuracy achievable in predicting the network response will be evaluated.

#### 3.1 Factors affecting the test network selection

There were several factors involved in forming the criteria for selecting a distribution line test network. Above all, it was deemed necessary that the network chosen was composed of lines constructed in accordance with utility standards regarding construction and materials. Besides adding weight to the data collected, actual distribution lines have peculiarities in their structure that may influence the results.

Since the test network would be used to test the mathematical model developed, the network must possess a tree structure topology. In addition, each section should have a length such that the transmission line effects discussed in Section 2 become prominent and can be observed and easily measured. At a DLC carrier frequency of 25 KHz, typical of that currently employed, a wavelength on an overhead distribution line is approximately 35,000 feet, or about six miles. Choosing an average length of each section of about a quarter wavelength, the total length of line required is then about 26,000 feet or about five miles.

Actual lines can be run overhead on utility poles, or can be buried underground. The modal parameters of these two configurations are very different hence it is necessary that the network selected is composed entirely of only one of these configurations. Of the two, the overhead

construction is desirable, since access to the conductors necessary for making signal measurements is unlimited. Underground lines, on the other hand, are obviously difficult to access.

Since the model was developed to predict the signal level in single-phase lines (e.g., one phase conductor and a neutral conductor), the network must be composed entirely of single-phase line sections. In addition, the presence of other parallel conductors (including other phase wires, telephone cables, etc.) in close proximity to the test lines should be avoided, as such conductors can alter the electrical characteristics of the test line.

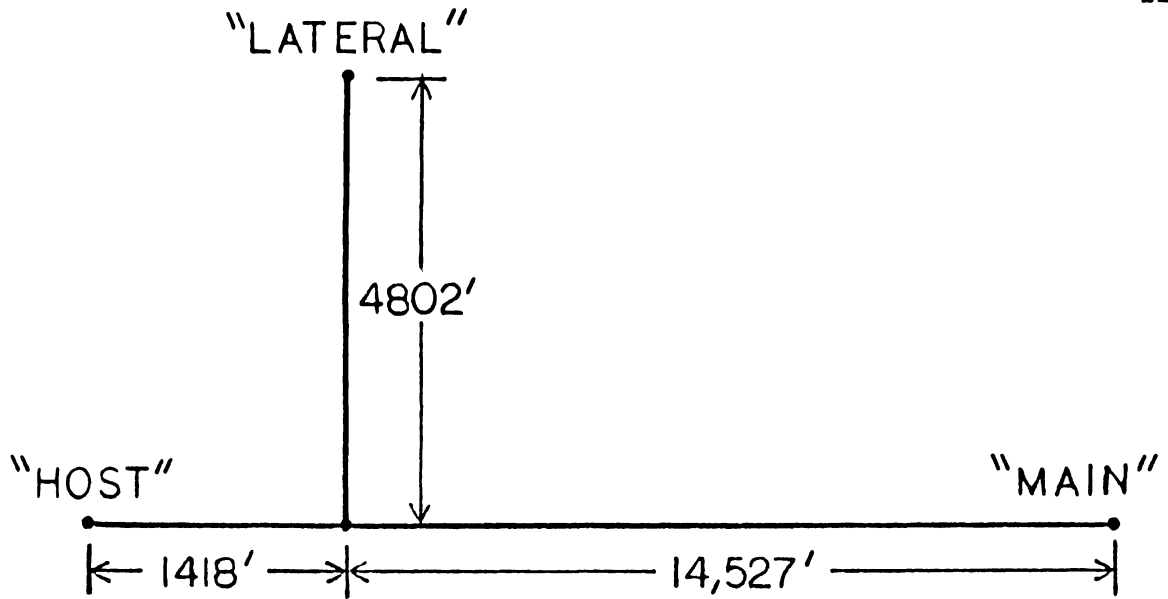
Because of the safety hazards involved in making direct measurements on energized (60 Hz) lines, it is also necessary that the test network can be de-energized during testing.

Unfortunately, the goal of selecting a test network currently in use by a utility is at odds with the realities of such lines. Most distribution lines are three-phase circuits; hence the criteria of using single-phase line sections is difficult to achieve, especially over the lengths required. Furthermore, de-energizing the lines would result in a temporary power outage to customers connected to the test network, a highly undesirable situation from a utility standpoint. There are other complications as well: few distribution lines in use are free of connections to equipment used by utilities for the efficient distribution of 60 Hz power, such as power-factor correcting capacitor banks, ratio banks, etc. Such equipment can affect signal propagation [CLI].

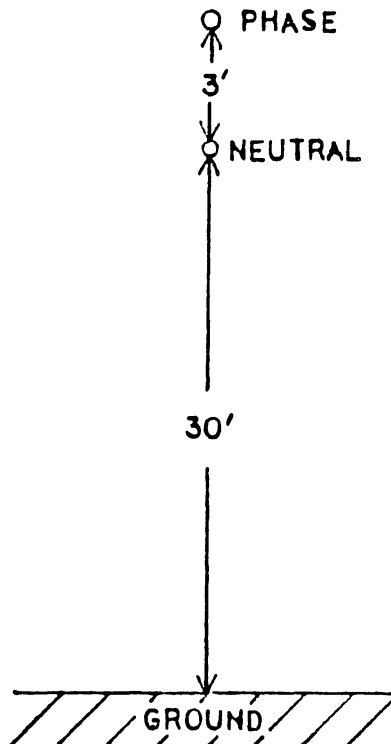
Because of the need to gather test data on distribution networks, and the difficulties of using actual lines as outlined above, Carolina

Power and Light Company has erected a system of simulated distribution lines. This facility, known as the Distribution Automation 23 KV Testbed, is located in New Hill, NC. It is composed of separate sections of single-phase and three-phase lines, which employ both overhead and underground constructions. The test facility lines are constructed according to CP&L's standards, and do not provide electrical service to any customers. In addition, the lines are constructed so that a variety of physical configurations are possible.

Only the single-phase, overhead section was utilized in these tests. This section has an overall length of 20,747 feet available for various configurations. Of the configurations available, the one chosen is depicted schematically in Figure 3.1.1. The network consists of a line section 1418 feet in length which is connected to a branch of two sections, one 14,527 feet long, and the other 4802 feet long. For identification purposes, three "ports", one at each of the free ends of the three line sections, are given titles (see Figure 3.1.1). Although these ports are depicted in Figure 3.1.1 as being separated, in reality all three are located physically at the same site (e.g., on the same utility pole). The significance of this arrangement will be discussed later (see section 4.4).



a) One-line diagram of test network, showing test ports



b) Vertical section of line, showing typical conductor spacing

FIGURE 3.1.1 Schematic of Test Network

#### 4. FIELD TESTS

Several sets of tests were conducted on the network described in Section 3.1. The test network was completely de-energized (60 Hz power) throughout these tests. The purpose, procedures and results of each test are described separately.

##### 4.1 Demonstration of symmetry of transfer impedance (Theorem of Reciprocity)

The theorem of reciprocity applies to passive, bilateral and linear networks. Networks which are "passive" are free from controlled, or active, sources. "Bilateral" implies the network is composed of components which have characteristics which are independent of the direction of current flow (e.g. non-polarized). "Linear" implies the network response is a linear function of the excitation. For example, assume the network response being measured is the voltage at a port in the network produced by a current (excitation) forced into another port of the network. Then, the response (output) can be described as

$$O = F(I) \quad (4.1.1)$$

where  $O$  is the response (output)

$I$  is the network excitation (input)

$F$  is the network function

If the network is linear, then any change in the input current should result in an equal change of the network response. Note

$$F(c \cdot I) = c \cdot F(I) = c \cdot O \quad (4.1.2)$$

where  $c$  is any constant.

If the output port is not loaded (open-circuited), the function  $F$  is just the open-circuit transimpedance.

The theorem of reciprocity states that the ratio of the voltage (open-circuit) developed at one port of a network to the current flowing into a second remains unchanged if the voltage is measured at the first port, and the current is flowing into the second. Stated differently, the impedance matrix of a linear bilateral network is symmetrical [PAR] . Reciprocity applies to any system of  $n$  ports,  $n$  being an integer greater than 2. Thus for any reciprocal  $n$ -port network,

$$Z_{ij} = Z_{ji} \quad i=j \quad (4.1.3)$$

where  $Z_{ij} = V_i / I_j$ ,  $I_i = 0$

Another condition that must be satisfied is that there exists no other sources elsewhere in the network, else they be disabled during measurement. This condition can be relaxed slightly by requiring that other sources that may be present in the network have no energy components of the same angular frequency as that of the excitation. The measurement of the network response must then be frequency selective.

The distribution network model meets the above conditions and hence it should be reciprocal between port pairs. By extension of the model, all distribution networks should also be reciprocal, regardless of the complexity of the path between port pairs. This, however, is sometimes difficult to envision, particularly when the network is complex and sprawling, and standing waves are present. A simple demonstration, using the test network, will confirm reciprocity does indeed apply for such networks.

One of the difficulties in making transimpedance measurements as described above is that the relative phase between the input and response cannot easily be established if the the two ports are separated appreciably. Therefore only the magnitude of the transimpedance can be measured. Since the transimpedance may be complex, it cannot be described by its magnitude alone.

This difficulty is avoided in the test network configuration by having all three ports concurrent. Thus both the magnitude and the phase of the transimpedance between port pairs can be measured and compared.

The equipment set-up used to measure the transimpedance between nodes of the test network is depicted in Figure 4.1.1. Current from the hp3570A Network Analyzer is allowed to flow into one network port. This current is varying in time sinusoidally with a frequency of 25KHz, and is measured (using a Tektronix P6201 AC Current Probe, equipped with a mV/2mA current-to-voltage converter) at channel A of the network analyzer. The voltage produced at another network node is measured at channel B of the network analyzer. The network analyzer channels have a high input impedance (> 1 Megohm). and as such should present negligible loading on the network. The response at channel B is thus the open-circuit voltage of that network node. The network analyzer is equipped with 100Hz-wide bandpass filtering on the front-end of the channels, and thus the measurements are frequency-selective.

This test was performed on each of the 3!=6 sets of port pairs. In addition, for each set-up, the current (excitation) magnitude was varied, and the network response measured and noted. This gives an indication of the network linearity.

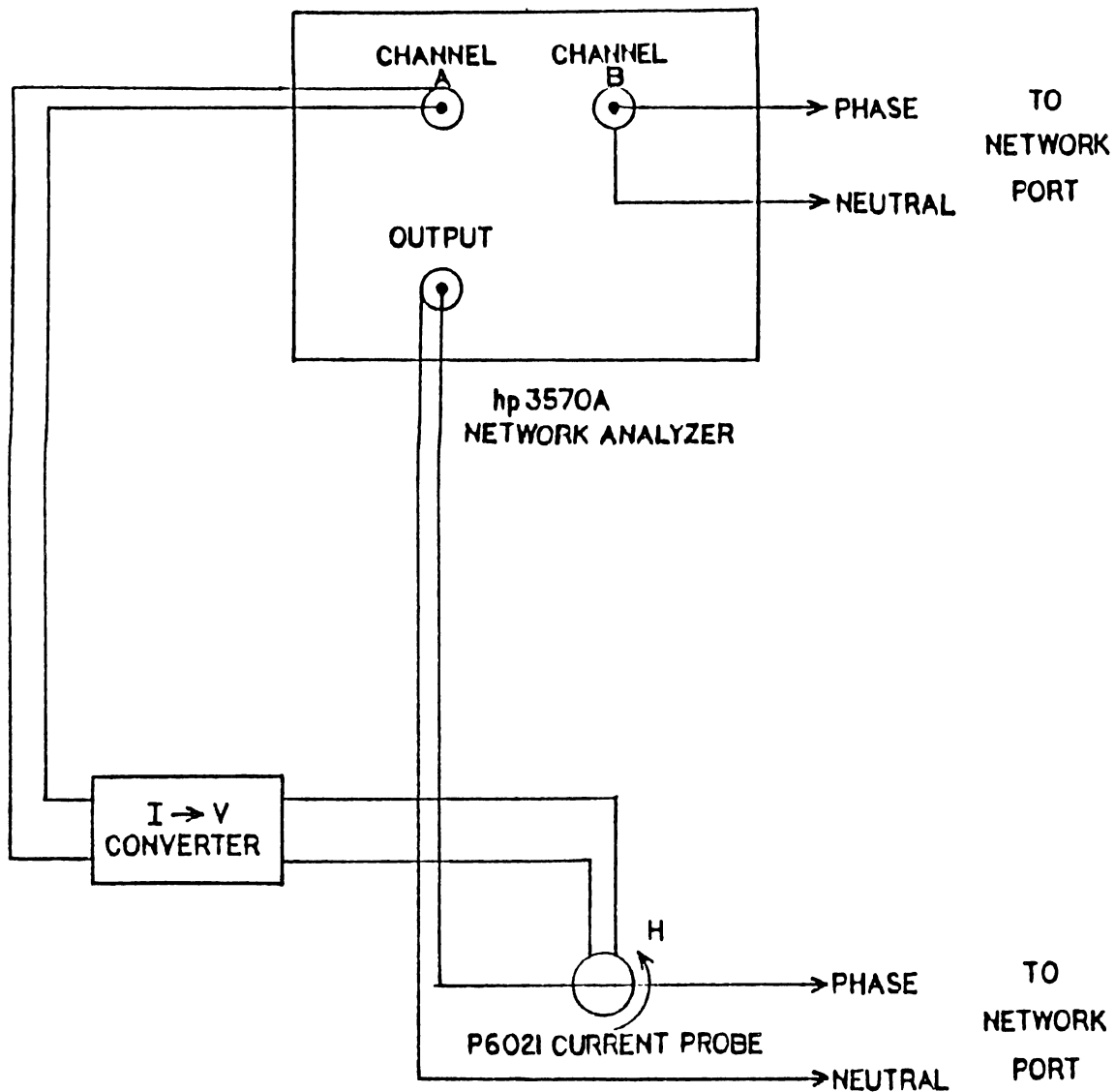


FIGURE 4.1.1 Equipment Test Set-up for Measuring Open-circuit Transimpedance.

TABLE 1 TRANSIMPEDANCE MEASUREMENTS

PORT 1: "HOST"

		PORT 2					
		"LATERAL"			"MAIN"		
		TRANSIMPEDANCE			TRANSIMPEDANCE		
INPUT ( $\mu$ A)	RESPONSE (mV)	MAGNITUDE (Kohm)	PHASE (deg)	RESPONSE (mV)	MAGNITUDE (Kohm)	PHASE (deg)	
575.5	707	1.227	-80	610	1.057	+103	
182.4	221	1.213	-80	191	1.057	+104	
56.4	70.0	1.256	-80	60.0	0.998	+104	

PORT 1: "LATERAL"

		PORT 2					
		"HOST"			"MAIN"		
		TRANSIMPEDANCE			TRANSIMPEDANCE		
INPUT ( $\mu$ A)	RESPONSE (mV)	MAGNITUDE (Kohm)	PHASE (deg)	RESPONSE (mV)	MAGNITUDE (Kohm)	PHASE (deg)	
571.5	697	1.213	-79	851	1.476	+103	
180.3	219	1.213	-79	269	1.476	+103	
56.4	69.0	1.213	-79	84.0	1.409	+103	

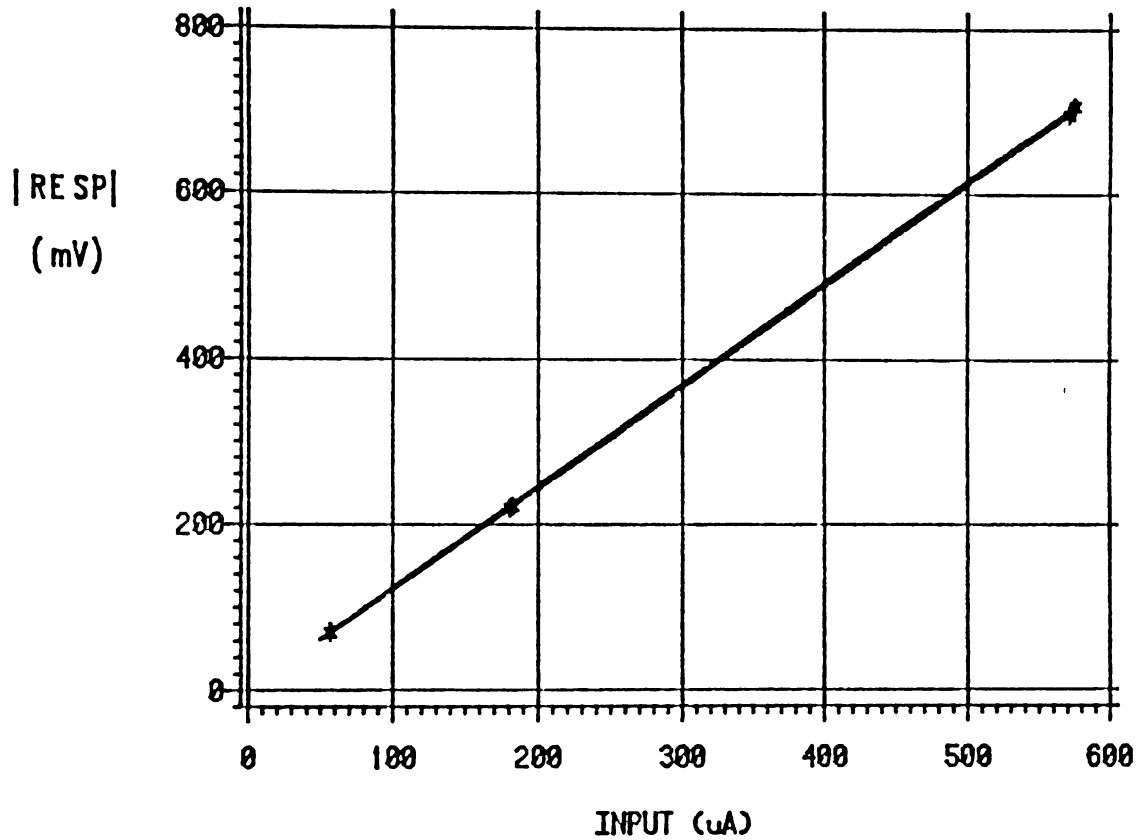
PORT 1: "MAIN"

		PORT 2					
		"LATERAL"			"HOST"		
		TRANSIMPEDANCE			TRANSIMPEDANCE		
INPUT ( $\mu$ A)	RESPONSE (mV)	MAGNITUDE (Kohm)	PHASE (deg)	RESPONSE (mV)	MAGNITUDE (Kohm)	PHASE (deg)	
576.8	856	1.476	+104	610	1.057	+105	
182.4	269	1.476	+103	193	1.045	+105	
56.4	84.0	1.409	+103	63.0	0.998	+104	

The results of the measurements are tabulated in Table 1. An examination of this table reveals that the magnitude and phase of the transimpedance between port pairs is identical when the source is at either port. Hence, the network is indeed reciprocal. In Figures 4.1.2-4.1.4, the response as a function of excitation is plotted for each set of port pairs. The plots are overlaid for the excitation at either port. The slope of the lines are the transimpedances between the ports. Since the lines are straight, this indicates the network is linear.

# NETWORK RESPONSE

measured between ports HOST and LATERAL

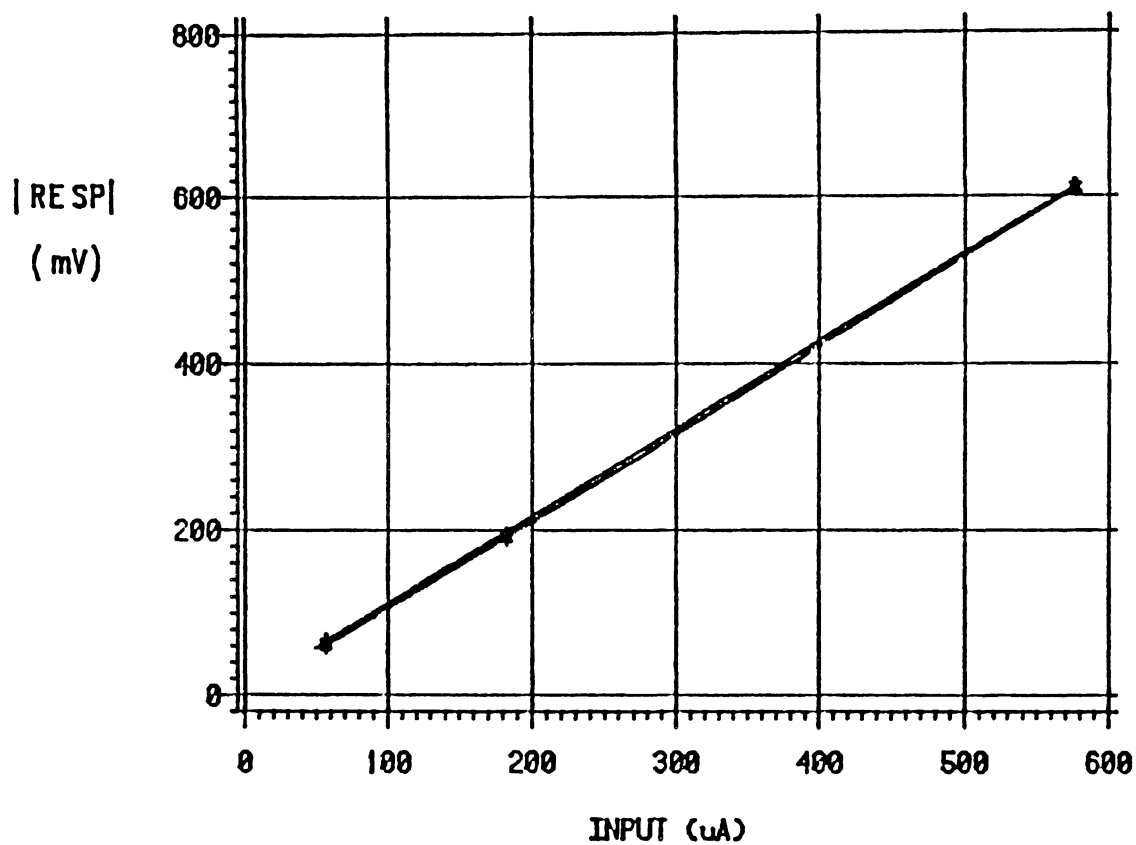


\* Source at HOST  
+ Source at LATERAL

FIGURE 4.1.2 Network Response Between Ports HOST and LATERAL

## NETWORK RESPONSE

measured between ports HOST and MAIN

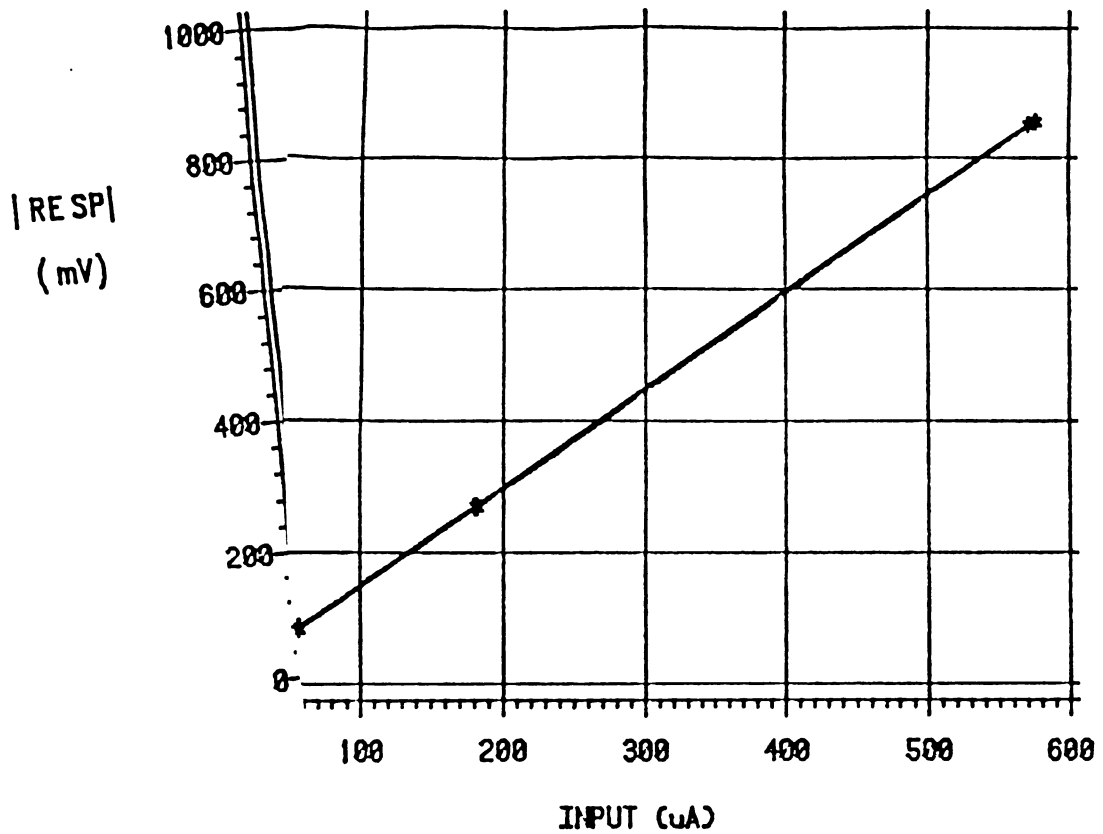


\* Source at HOST  
+ Source at MAIN

FIGURE 4.1.3 Network Response Between Ports HOST and MAIN

# NETWORK RESPONSE

measured between ports LATERAL and MAIN



\* Source at LATI  
+ Source at MAI

FIGURE 4.1.4 Response Between Ports LATERAL and MAIN

## 4.2 Measurements of signal propagation in the test network

The objective of these tests is to gather data on a physical network which will be compared to data generated by the simulation program. This will verify the assumptions used in making signal propagation calculations, and provide an indication of the accuracy achievable.

The equipment set-up for all tests is depicted in Figure 4.2.1. The hp3570A Network Analyzer ( with hp3330B Automatic Synthesizer) generates a low-level sinusoidal signal. The frequency of the signal was adjusted to 25Khz. This signal is fed into an hp467A Power Amplifier, which amplifies the signal and provides a low-impedance output (<10 ohms) with which to drive the network. At the output of the amplifier is a switch which selects one of two series impedances, a 470 ohm resistor and a 100 ohm resistor, that connect the amplifier to the phase conductor of one port of the network. The common side of the equipment is connected to the neutral conductor of this same port. The current entering the network is measured using a Tektronix P6021 AC Current Probe equipped with a mV/2mA current-to-voltage convertor, which is connected to the channel A input of the network analyzer. The network analyzer has a 100Hz-wide bandpass filter at its inputs.

The signal generator was adjusted to provide maximum output of the hp467A Power Amplifier without distortion. This level was maintained constant throughout each test conducted.

In the first test, the port identified as "HOST" was used as the input port. The voltage magnitude produced between the phase and neutral conductors was measured at 31 points throughout the network. A

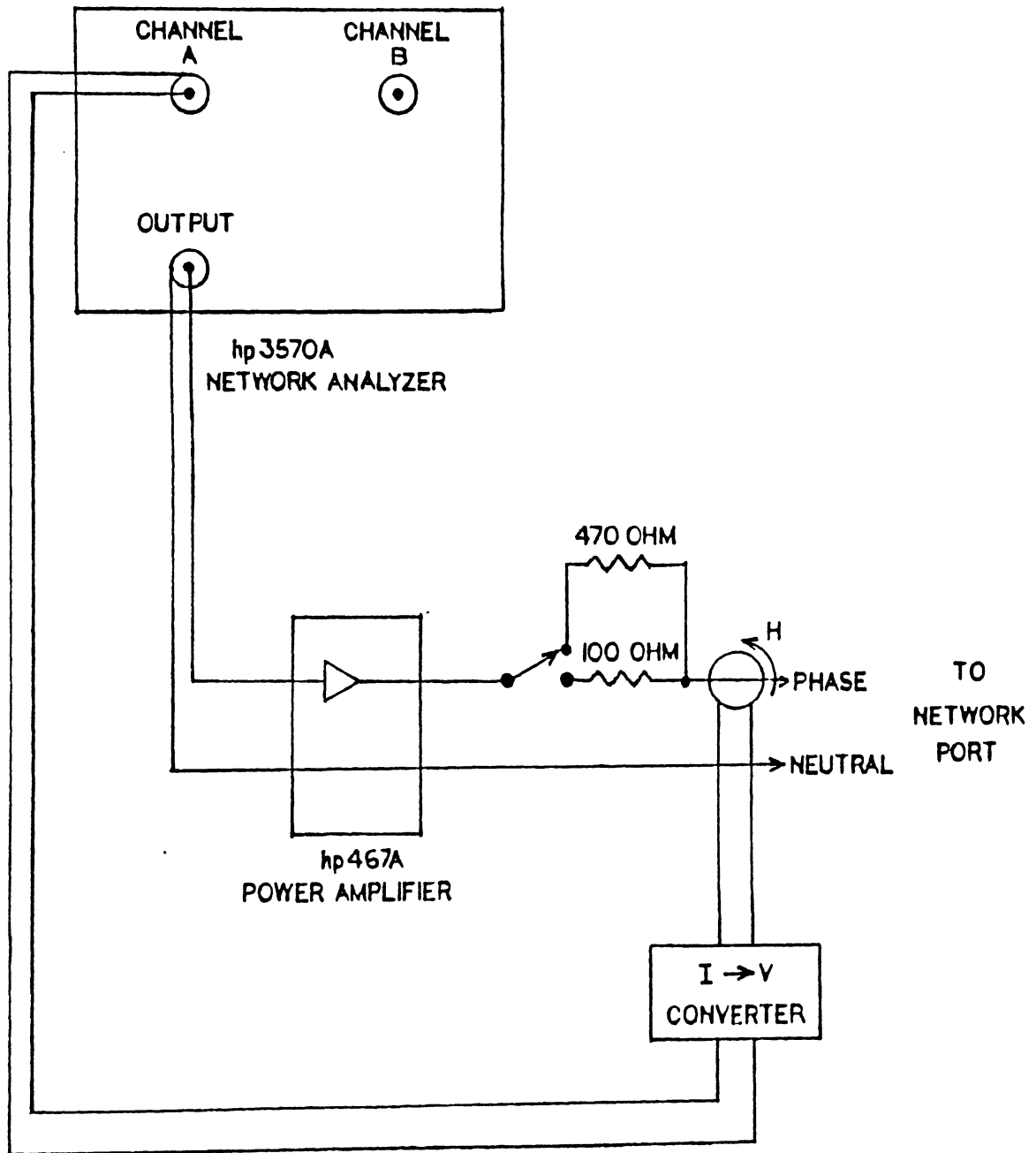


FIGURE 4.2.1 Equipment Test Set-up

Showing equipment used to drive network during signal propagation measurements.

bucket truck was used to gain access to the conductors. The points were chosen to be very nearly equally spaced, and the locations coincided with the utility poles supporting the conductors. The phase-to-neutral voltage (network response) was measured using a Tektronix Model 212 Portable Oscilloscope. The measurements were made at each of the 31 points while the 470 ohm series impedance connected the source to the network, and again with the 100 ohm series impedance selected. The current into the network was also recorded during each measurement.

The results of these measurements are plotted in Figures 4.2.2. The response (voltage from the phase to neutral conductors) at the 31 test points is plotted as a function of network distance from the source, for both values of source impedance. The points are connected to form a continuous curve, using a smooth line generated with a spline function.

There are several notable observations in the network response shown in Figure 4.2.2. First of all, the voltage is observed to rise to a maxima at the end of each section terminated in an open circuit (these points are nodes "LATERAL" for the shorter section, and "MAIN" for the longer). This is a well known fact from transmission-line theory of low-loss lines. Furthermore, there is a very noticeable minima in the response pattern at about 6500 feet from the source on the longer branch section. This minima is induced by total reflection of the voltage wave from the open circuit at the end of the longer branch section. From transmission-line theory, this minima must be located a quarter-wavelength from the end of the line (see equation (2.3.3)).

Also note the network response is continuous in the region of the branch, an assumption pointed out in Section 2.2.

# NETWORK RESPONSE

variable source impedance

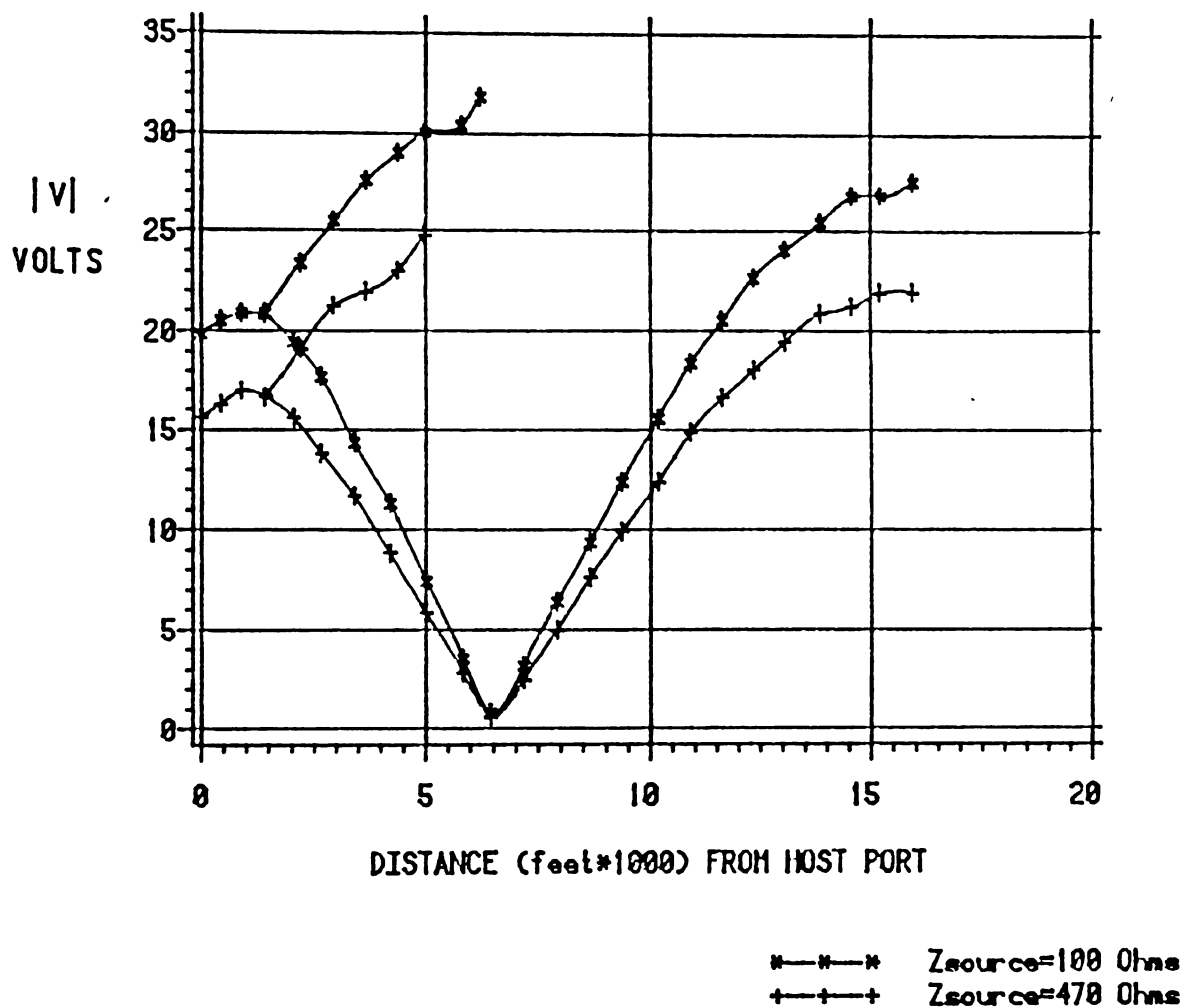


FIGURE 4.2.2 Measured network response vs. distance from source, for two values of source impedance.

Source located at HOST port.

The response is observed to have a similar "shape" for both cases of source impedance - that is, points of relative and absolute extrema coincide, and the functions exhibit the same regions of increase and decrease. In short, the two plots of network response appear to be scaled versions of each other, with the response in the case of the 100 ohm series impedance everywhere greater than that for the 470 ohm series impedance case.

These results are easily explained. The network has a given input impedance, which can be calculated using equation (2.1.9). The source exciting the network the network will deliver more current into this impedance, and hence into the network, with a lower series impedance connecting it to the network. This was indeed the case, as was seen by examining the measurements that were made of input current during the field measurements. Therefore, the network excitation (input current) will be greater when the 100 ohm series impedance is used than when the 470 ohm series impedance is used. The increased input current in the 100 ohm case will result in a proportionately increased network response everywhere in the network, the constant of proportionality being the transimpedance.

The magnitude of the network transimpedance between the source node and each of the test points has been calculated, and the results are plotted in Figure 4.2.2. The transfer impedance magnitude is calculated as

$$|Z| = |V_i| / |I_s| \quad (4.2.1)$$

where  $|Z|$  is the transimpedance magnitude

# NETWORK TRANSIMPEDANCE

variable source impedance

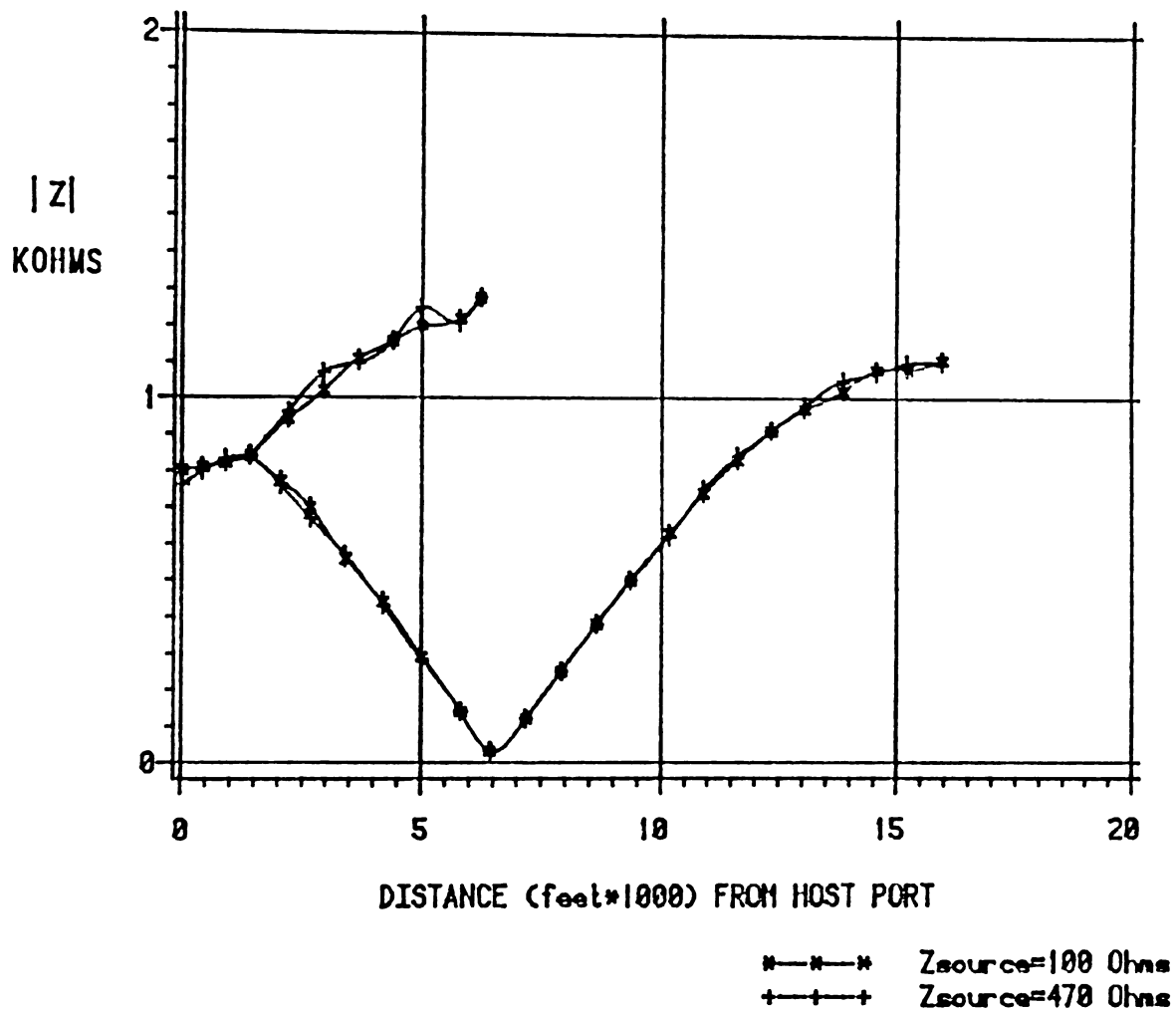


FIGURE 4.2.3 Network transimpedance calculated from measured data for two values of source impedance.

Source located at HOST port.

$|V_i|$  is the magnitude of the voltage  
at test point  $i$

$|I_s|$  is the magnitude of the source  
current

The network transimpedance is seen to be the same at all points in the network for both cases of series impedance. This can be generalized for all values of source impedances. Thus, as stated in Section 2.3, the source impedance has no effect on the network transimpedance.

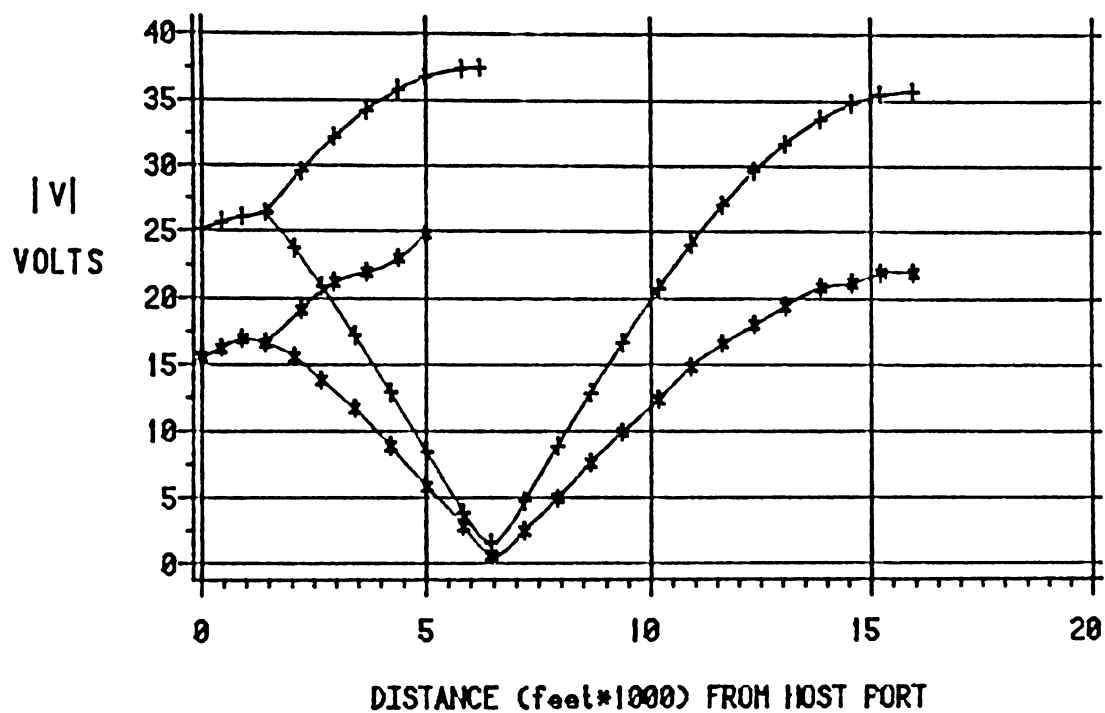
In Figure 4.2.4, the measured values of network response with the series impedance of 470 ohms are plotted along with the response predicted at each of the test points using the computer program discussed in Section 2.4. The mean value of the network input current measured during field tests was used as the source current in the simulation program.

Examining Figure 4.2.4, it appears the predicted and measured values produce curves of the same shape. Therefore, the program was accurate in predicting the location of response extrema. This is valuable, since the points of response minima correspond to points at which communication is degraded. However, the predicted values appear to be in error by about +60% at all points. This is far greater than the amount that can be attributed to measurement error, which is estimated at about 5%. Clearly, this significant difference in predicted and measured values must be accounted for if the model is to be used with confidence.

Since it appears the two curves differ by only a "scaling factor", it was initially surmised a portion of the measured source current was somehow diverted and never entered the network. As just pointed out, a

## NETWORK RESPONSE

measured and predicted



\*—\*—\* MEASURED  
 +—+—+ PREDICTED

FIGURE 4.2.4 Measured and predicted network response with 470 ohm source impedance.

Plotted as a function of network distance from the source, source located at HOST port.

reduction in the network input current causes a proportionately lower response everywhere in the network. Several attempts were made to isolate and identify such a diversion path and bring the measured values within closer agreement with the predicted values. These attempts included the use of an isolation transformer to power the test equipment and provide assurance there existed no metallic path between the equipment chassis and the supply ground. Furthermore, the source current was measured, using a clamp-on current probe assembly, along the entire path leading from the source, through the lead-in wires and onto the network conductors, to detect any diversion of the source current. All resulted in a failure to uncover any such diversion path. It was assumed the measurements were valid and being made correctly, and hence testing continued.

On the assumption the measured values are indeed correct, it is apparent the error is due to some parameter or combination of parameters in the prediction model. The most likely candidates are the modal parameters. Consider the line characteristic impedance first. The impedance into a line section is directly proportional to the line characteristic impedance for a given length of line section and termination (see equation (2.1.9)). Therefore, a discrepancy between the actual and calculated characteristic impedance use in the model could result in an error between the actual and predicted input impedance to the network. By equation (2.1.8), such an error would also affect the voltage  $V_0$  at the source end of the network, and in turn the arbitrary constants  $V_+$  and  $V_-$  (see equation (2.1.3)). However, because of the one-to-one relation between the input impedance and the characteristic impedance, the calculated

characteristic impedance must be in error by at least 60% to fully explain the error observed in the predicted network response. The calculated line characteristic impedance is not believed to be in error by this amount (see Section 4.3, where the network is terminated into its characteristic impedance).

Next, consider the propagation constant, which is complex and can be expressed as

$$c = a + jb \quad (4.2.1)$$

where  $c$  is the propagation constant

$a$  is the attenuation constant

$b$  is the phase constant

Rewriting equation (2.1.2) by expanding the propagation constant yields

$$V(z) = V_+ \exp(-az) \exp(-bz) + V_- \exp(az) \exp(bz) \quad (4.2.2)$$

Note the forward wave is attenuated as distance increases from the source, while the reflected wave is attenuated as it travels away from the load ( $-z$  direction). Therefore, while increasing the attenuation constant will reduce the response at some points throughout the network, the shape of the response will also vary. In particular, where the forward and reflected waves are out-of-phase 180 degrees (creating signal nulls) the cancellation becomes less pronounced as the attenuation constant is increased. In addition, the signal peaks which occur when the forward and reflected waves are in-phase will not be as large, particularly when the peaks occur close to the source. In conclusion, it is not believed the error is due to discrepancies in the actual and calculated

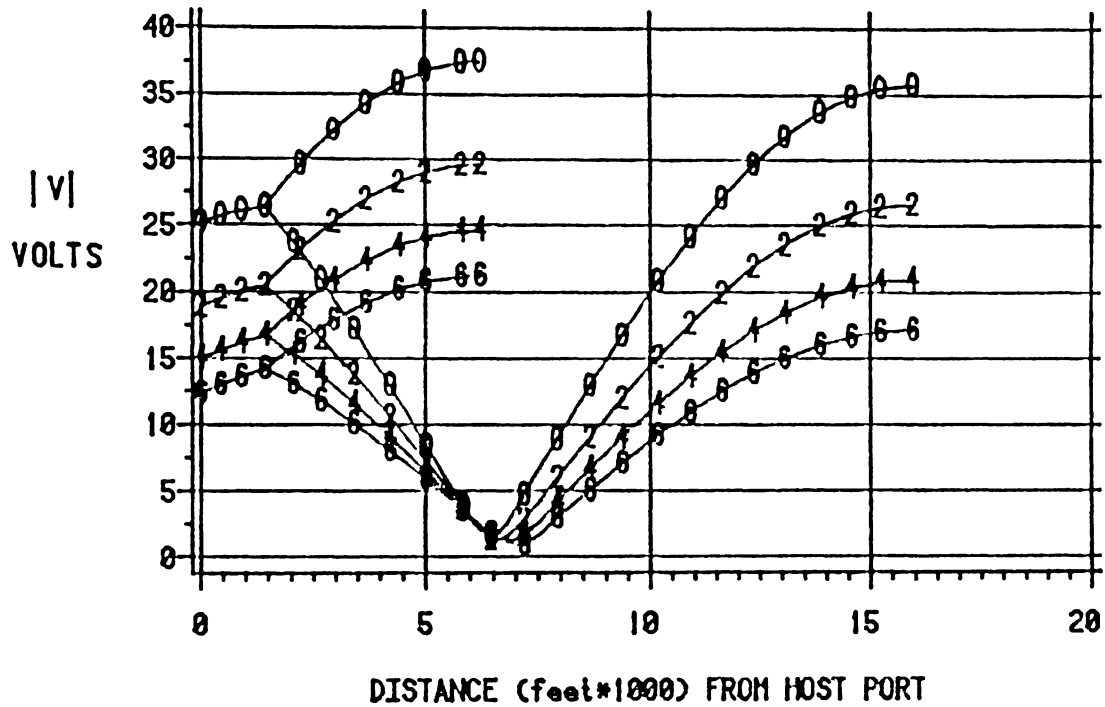
attenuation constant.

Focusing on the phase constant, it is clear from equation (2.1.1) that a change in the phase constant will affect the shape of the response curve by altering the location of the response extrema; that is, where the forward and reflected waves are in-phase or out-of-phase. Since the measured and predicted curves appear to differ only by a scale factor, the phase constant does not seem to be a likely source of error in the two curves. However, upon closer examination of Figure 4.2.4, it is noted that both curves do not exhibit the same shape in the region of the null at 6500 feet from the source on the longer branch. This is illustrated in Figure 4.2.5 where a line has been drawn through each of the two values on either side of the nulls. Notice the slope of the line is positive for the predicted values, and negative for the measured values. A mere scale factor would not cause this change. More likely, the nulls occur at different points in the two curves. The actual location of each of the nulls is not identifiable since the finite set of points plotted probably does not include the minima; the actual minima have been "smoothed over" by the curves.

Clearly, all of the error between the measured and predicted values cannot be explained by a "shifting" of the curves due to a small change in the phase constant. However, it is conceivable some other network parameter is "sensitive" to changes in the phase constant and may indirectly affect the network response significantly. To investigate this, a family of network response curves was generated by the simulation program using variations in the phase constant. The results are plotted in Figure 4.2.6.

# NETWORK RESPONSE

variations in phase constant



0--0--0     $b=+0\%$  (ref)  
 2--2--2     $b=+2\%$   
 4--4--4     $b=+4\%$   
 6--6--6     $b=+6\%$

FIGURE 4.2.6 Predicted network response with 470 ohm source impedance, for five values of phase constant.

Plotted as a function of network distance from the source, source located at HOST port.

It is evident a small change in the phase constant results in dramatic changes in the predicted network response, at least for this network configuration. Hence, the network response is very sensitive to the phase constant, where sensitivity is defined formally as [DAV]

$$S = \frac{x}{N} \frac{dN}{dx} \quad (4.2.3)$$

where  $S$  is the sensitivity of a network function  $N$  to a change in some parameter  $x$  of the network.

In figure 4.2.7, the network input impedance has been calculated for each value of the phase constant from Figure 4.2.6, and plotted as function of the phase constant. It also appears the input impedance is very sensitive to variations in the phase constant, and this results into large errors in the predicted values of the arbitrary constants  $V^+$  and  $V^-$  (see equations (2.1.8) and (2.1.3)) and hence the overall network response.

Therefore, it appears the error in the prediction of the network response is due to a slight error in the phase constant used in the program. To "calibrate" the model, a value of the phase constant which yields a predicted input impedance close to that measured was selected (see Figure 4.2.7), and the program was executed again to yield a new predicted network response. This is plotted along with the measured network response in Figure 4.2.8. In this plot, the error due to the incorrect phase constant is factored out, and the residual error appears small.

Throughout the remainder of this paper, a modified phase constant (denoted as  $b'$ ) will be used. From Figure 4.2.7,

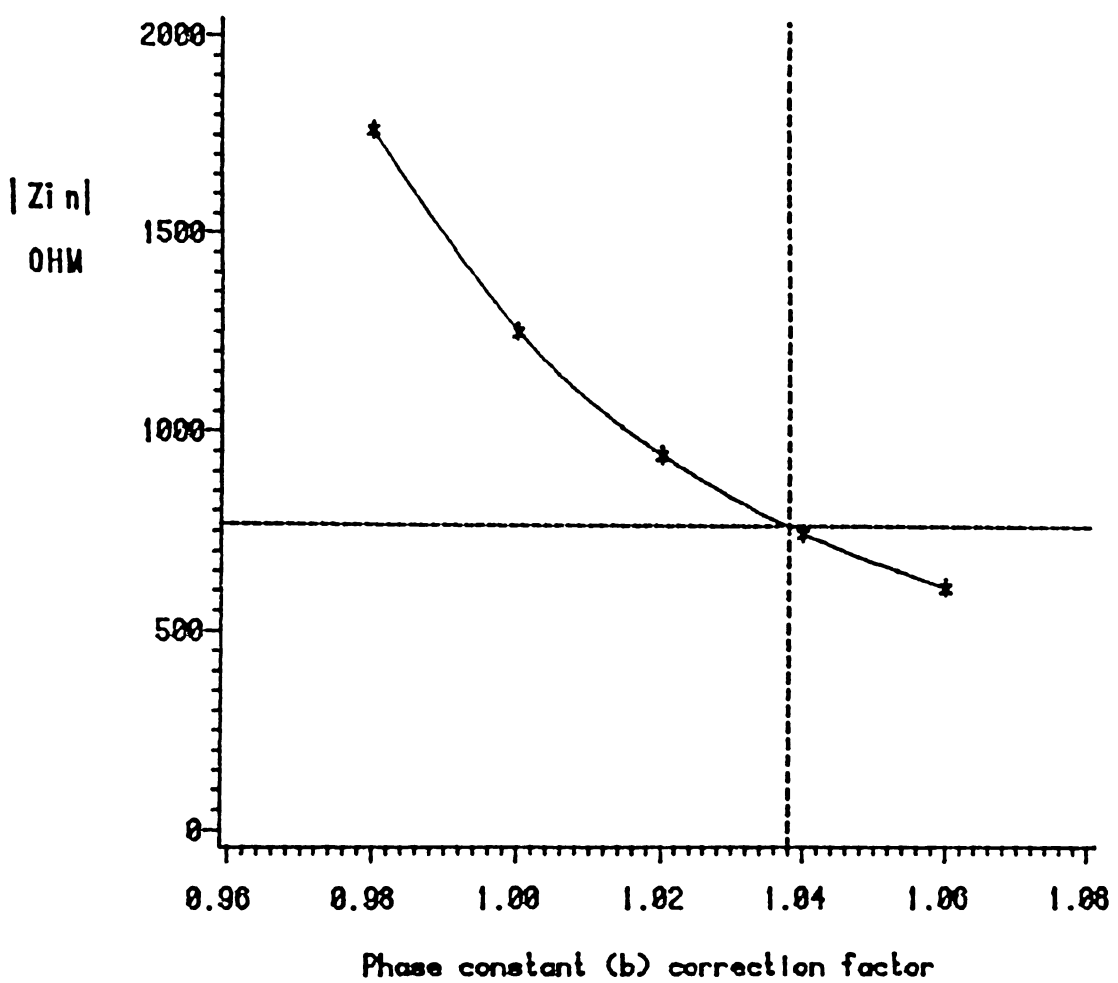
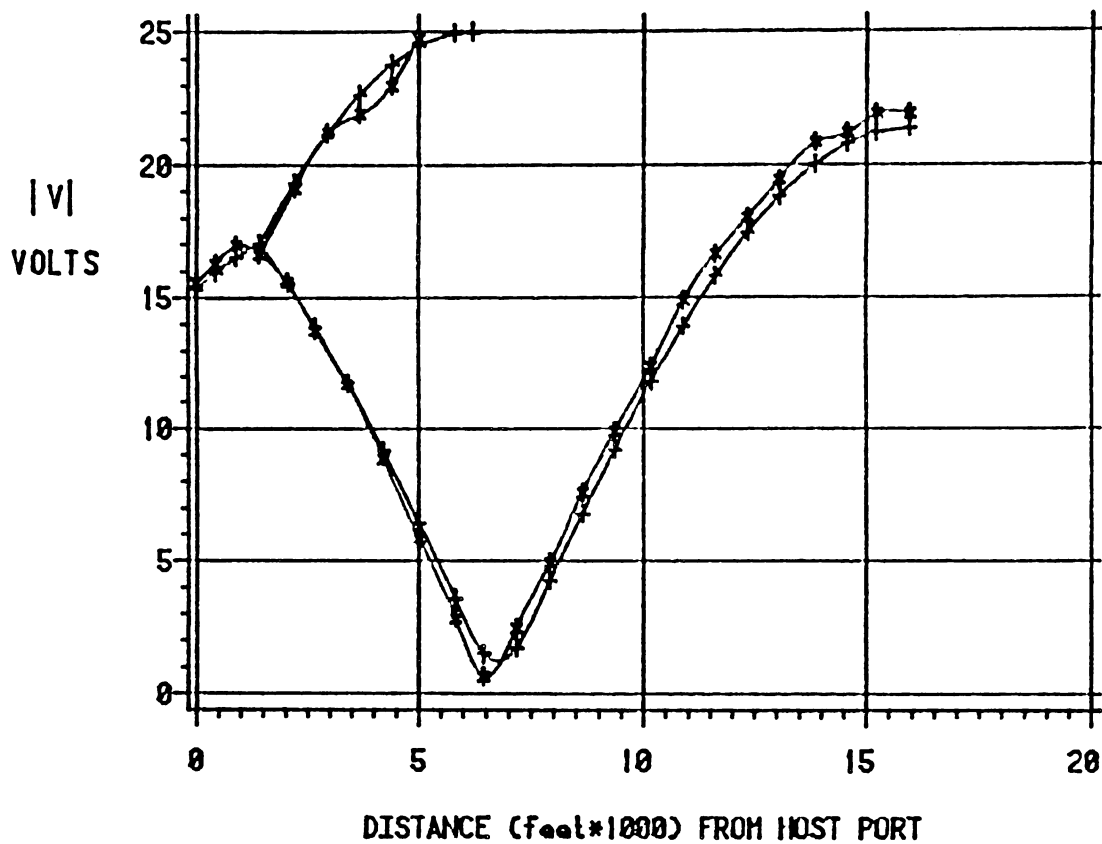


FIGURE 4.2.7 Predicted values of HOST port input impedance ( $Z_{in}$ ) for variations in phase constant.

Lines intercepting plot indicate measured value of input impedance, and model correction factor.

# NETWORK RESPONSE

measured and predicted



\*-\*- MEASURED  
+--+ PREDICTED

FIGURE 4.2.8 Measured and predicted (using modified phase constant) network response with 470 ohm source impedance.

Plotted as a function of network distance from the source, source located at HOST port.

$$\begin{aligned} b' &= 1.02 * b \\ &= f*b \end{aligned} \quad (4.2.4)$$

Note when the attenuation constant becomes negligible, equation (2.1.1) becomes

$$V(z) = V+\exp(b'z) + V-\exp(b'z) \quad (4.2.5)$$

$$= V+\exp(b*f*z) + V-\exp(b*f*z) \quad (4.2.6)$$

$$= V+\exp(b*z') + V-\exp(b*z') \quad (4.2.7)$$

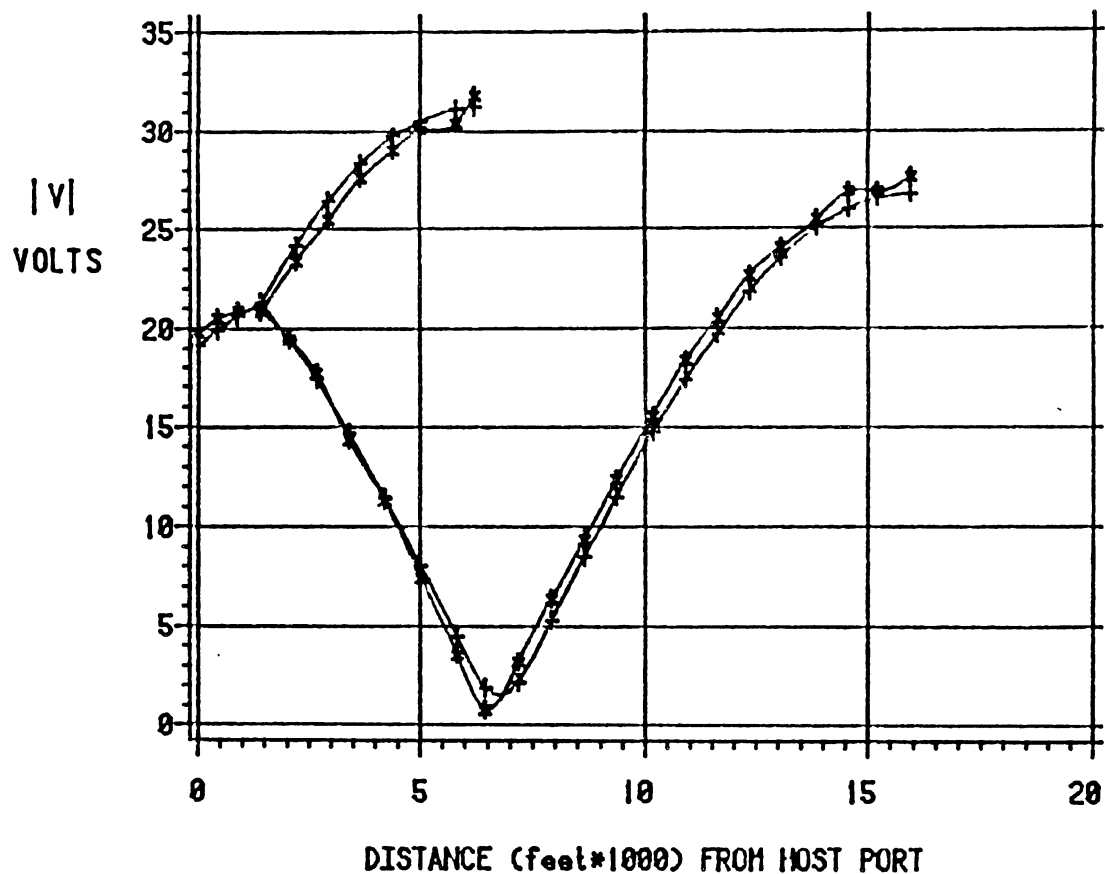
where  $z' = f*z$

Therefore it appears a small change in the measurement of the line lengths could affect the predicted network response the same as an error in the phase constant; hence, the source of error is indistinguishable. Errors in line measurements could arise from the difficulty in making accurate measurements over rough terrain, unaccounted line sag, differences in the length of the line span and pole spacings due to insulators, etc. Quite possibly the error is due to a combination of errors in line measurements and calculation in phase constant. To maintain a common coordinate system with which to compare measured and predicted values, all of the error will be "lumped" into the phase constant.

Figure 4.2.9 shows plots of measured and predicted (using the modified phase constant) values of network response, when the network is connected to the source through a 100 ohm series impedance. The agreement is good.

# NETWORK RESPONSE

measured and predicted



\*-\*- MEASURED  
+--+ PREDICTED

FIGURE 4.2.9 Measured and predicted (using modified phase constant) network response with 100 ohm source impedance.

Plotted as a function of network distance from the source, source located at HOST port.

#### 4.3 ARTIFICIAL LOADING TO IMPROVE NETWORK RESPONSE

Examining the response throughout the network plotted in Figure 4.2.1, a very marked null in the signal is apparent at about 6500 feet from the source on the longer branch. As mentioned above, this is a low (line) impedance point due to total reflection of the voltage wave at the open circuit at the end of that section. Since the DLC remote receivers respond to the line voltage of the DLC signal at their locations, receivers located in the vicinity of such nulls may exhibit marginal performance. The receivers may not respond at all if the signal level is below the receiver sensitivity. If, on the other hand, the signal level is above the receiver sensitivity, but the in-band noise is high at such nulls, the received signal-to-noise ratio (SNR) may be too low for reliable communications. Furthermore, by reciprocity, current injected into the network at such locations of low line impedance will also result in low received voltage at the substation, where bidirection systems are employed.

Clearly, the occurrence of such nulls can be a limiting factor in the performance of the system. Efforts to improve communication to such points include the following approaches [ONE]:

- i.) Placing repeaters throughout the system. The repeaters are intended to improve the inbound communication (transmission from remote units to the central unit) through the use of spatial diversity. An algorithm for the placement of repeaters does not currently exist, however. There is no guarantee that installing a repeater will improve the inbound

communication of all remote units. Furthermore, the repeaters introduce a delay in the transmission of data that can reduce the throughput of the system.

- ii) Transmitting a number of carrier frequencies. This is another form of spatial diversity. However, it increases the complexity of the receiver design.

Voltage nulls may also be reduced or eliminated by terminating the lines into an impedance equal to the characteristic impedance of the line. This in effect eliminates reflection of the voltage wave traveling toward the end of the line (Note  $p=0$  in equation (2.1.12) when  $Z_1=Z_0$ ). The voltage everywhere along the line has a magnitude very nearly  $|V^+|$  when the line losses are low (equation (2.1.1), with  $V^- = 0$ ).

The elimination of reflections at the end of a transmission line is desirable when a single line is connecting a source to a load. This is because the energy reflected from the load when it is not "matched" to the line represents a loss of efficiency in delivering power to the load. Therefore, the idea of terminating the distribution line with the line characteristic impedance seems obvious. Unfortunately, distribution networks are not characterized as single lines, but as networks of branches. The problem of providing a "match" in branched networks is not considered often in practice. (One noticeable exception is the use of a "stub" section to "match" an otherwise mismatched load. The goal of this approach is to achieve the maximum transfer of power from the source to the load. The "loads" in a DLC system do not all occur at the end of the lines, but instead are dispersed throughout the system of lines. The distribution of line voltage is not usually considered when using "stub tuning". In

fact, standing waves are generated on the lines, so the voltage nulls are not eliminated by any means in this approach)

To understand the difficulties inherent in attempting to match a network with branches, consider the simple example of the test network. Matching each branched section by placing an impedance equal to the line characteristic impedance at nodes "LATERAL" and "MAIN" would eliminate reflections from the end of these sections. The input impedance to each section will also equal the line characteristic impedance. However, the impedance seen at the end of the section feeding the branch will be  $Z_0/2$ , hence a portion of the forward wave on that section will be reflected.

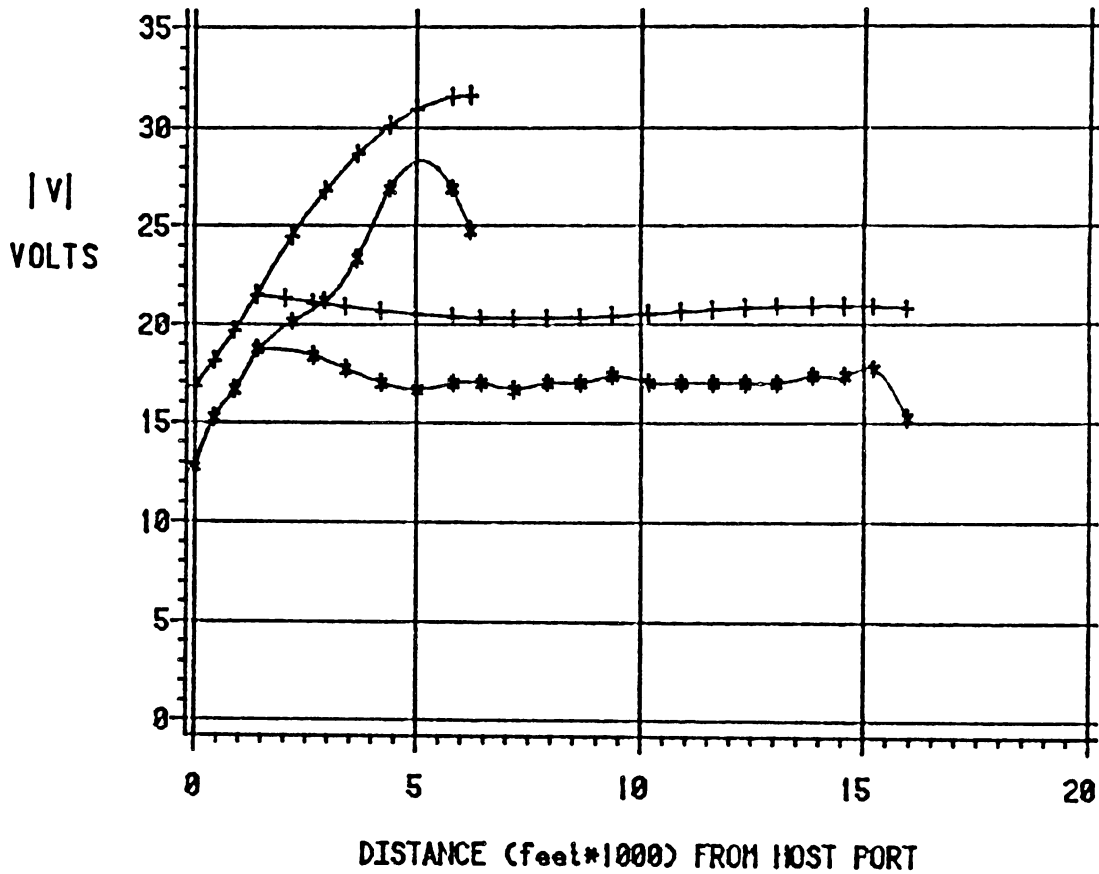
It is apparent an overall match cannot be achieved in distribution line networks. However, this approach can still have merit. Notice in Figure 4.2.1 that a voltage null exists only on the longer branch. Indeed on the shorter branch, the voltage is increasing monotonically toward the line end. Therefore, there seems to be no need to terminate such a section into its characteristic impedance, unless the section was so nearly a quarter-wavelength long that the resulting low input impedance of that section shorted out the remainder of the network.

A practical application of this approach is to terminate each line section that is near a quarter wavelength or longer with its characteristic impedance.

This approach was applied to the test network. An impedance close in value to the characteristic impedance of the lines was connected to node "MAIN". The network response was again measured, as outlined in Section 4.2. The results are plotted in Figure 4.3.1. In Figure 4.3.2,

# NETWORK RESPONSE

measured and predicted



\*-\*- MEASURED  
+--+ PREDICTED

FIGURE 4.3.1 Measured and predicted network response for a loaded network, as a function of distance from source, source located at HOST port.

# NETWORK TRANSIMPEDANCE

measured and predicted

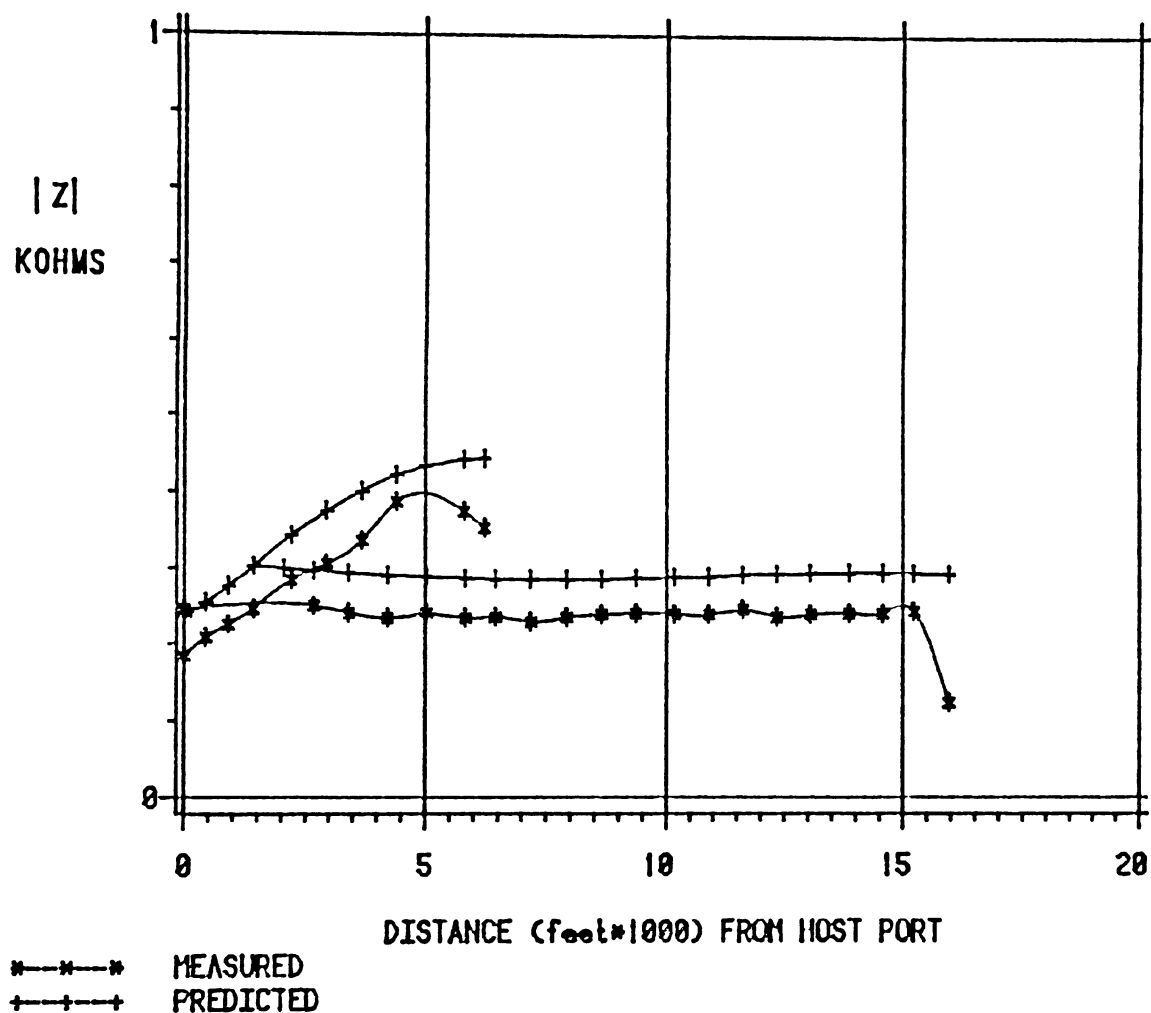


FIGURE 4.3.2 Measured and predicted network transimpedance for a loaded network. Distances from source, source located at HOST port.

the network transimpedance is plotted, and in Figure 4.3.3, the transimpedance of the terminated line is plotted against that of the unterminated line.

As expected, the network response along the longer branch section is nearly constant with a slight attenuation noticeable. (The significantly lower measured value at the end of that line is attributed to measurement error). In addition, the response is increasing toward the end of the shorter, unloaded line. (Again, the significantly lower measured values at the end of that line are attributed to measurement errors).

It is obvious from the plots that the single termination has eliminated the voltage null which was present on the unterminated network. However, as evident in Figure 4.3.3, the termination has significantly reduced the network transimpedance. Thus, while the use of the termination may work to the benefit of a few receivers, it has an overall adverse effect.

# NETWORK TRANSIMPEDANCE

unloaded and loaded networks

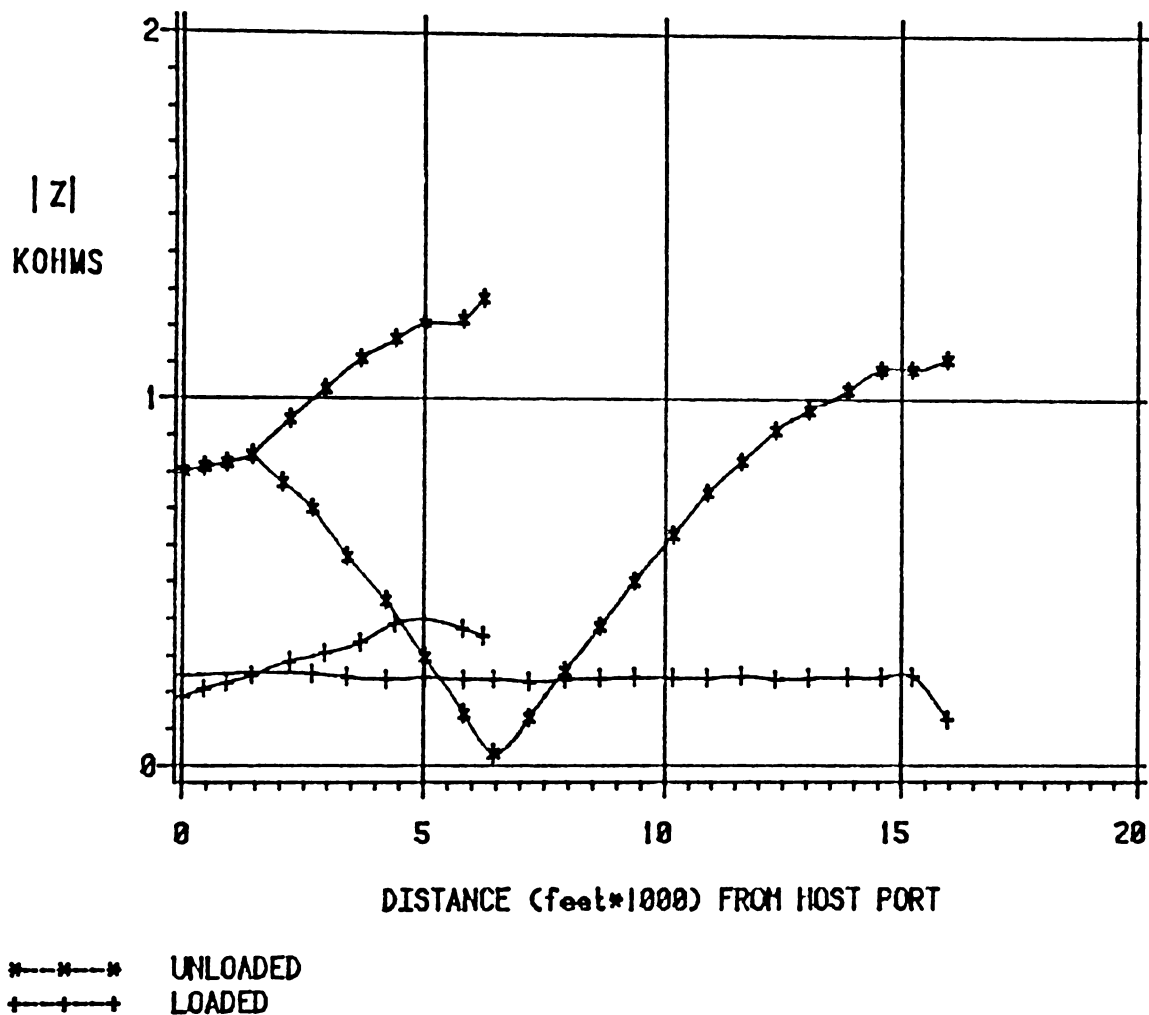


FIGURE 4.3.3 Measured network transimpedance for loaded and unloaded networks.

Distances from source, source located at HOST port.

#### 4.4 Simulation of noise profile

Sources of noise in distribution networks are generally believed to originate from the secondary of distribution transformers. Electric motors, SCR switching devices are examples of equipment connected to the secondary of the distribution transformers that generate noise with a magnitude spectrum extending up to typical DLC frequencies [VIN]. This noise is coupled onto the distribution network through the distribution transformer. Since the primary side of the distribution transformer approximates an ideal controlled current source (controlled by the voltage at the secondary), noise sources can be modelled as current sources [SHU].

These sources of noise are scattered throughout the network; that is, noise current is injected into a large number of ports. There is a transimpedance associated with each port at which the noise is injected and the voltage developed at all other ports. This resulting voltage from all noise sources is the noise voltage at each port which the DLC signal must overcome.

When the DLC system is narrowband, the noise magnitude spectrum of interest is mainly near the DLC carrier frequency. What is of interest in noise analysis is the magnitude of voltage produced throughout the network due to a remote (noise) current source. In particular, does the same "pattern" of response result independent of position of the source in the network? If so, it stands to reason that the signal-to-noise ratio will be a constant insofar as outbound communication is considered, when the noise originates from a single predominant source. If this is not the case, the SNR will be a function of position in the network, and

points of low received signal level may also have a very poor SNR.

When the noise is due to contributions from several sources in the network, the noise voltage produced by each must be considered. Since the network is linear, the principle of superposition can be applied to evaluate the overall noise voltage distribution. The noise voltage at any location is simply the sum of the voltages produced by all the sources considered one at a time. Here again, the distribution of noise voltage relative to that of the signal is of interest.

To gain some insight into these questions, several signal propagation measurements were again taken at the test facility. The first set employed the test procedure outlined in Section 4.2. However, this time the source was connected first to the LATERAL port using a 100 ohm series impedance. The response throughout the network was again measured. Then, the source was connected to the MAIN port, and the network response measured. In both cases, only the 100 ohm series impedance was used to connect the source to the network.

The results of the measurements, with the source at the LATERAL port are plotted in Figure 4.4.1, with the network response a function of distance from the source. In this configuration, the network looks like a single line 4820' long connected to the source (at the LATERAL port) and feeding a branch. The branch is made up of a shorter (1418') section that ends at the HOST port, and a longer branch that ends at the MAIN port. The branched sections are terminated into an open-circuit. In Figure 4.2.2, the network transimpedance has been calculated from the measured data, and plotted against the values predicted using the program.

The same procedure was followed for the case of the source connected

# NETWORK RESPONSE

source at LATERAL

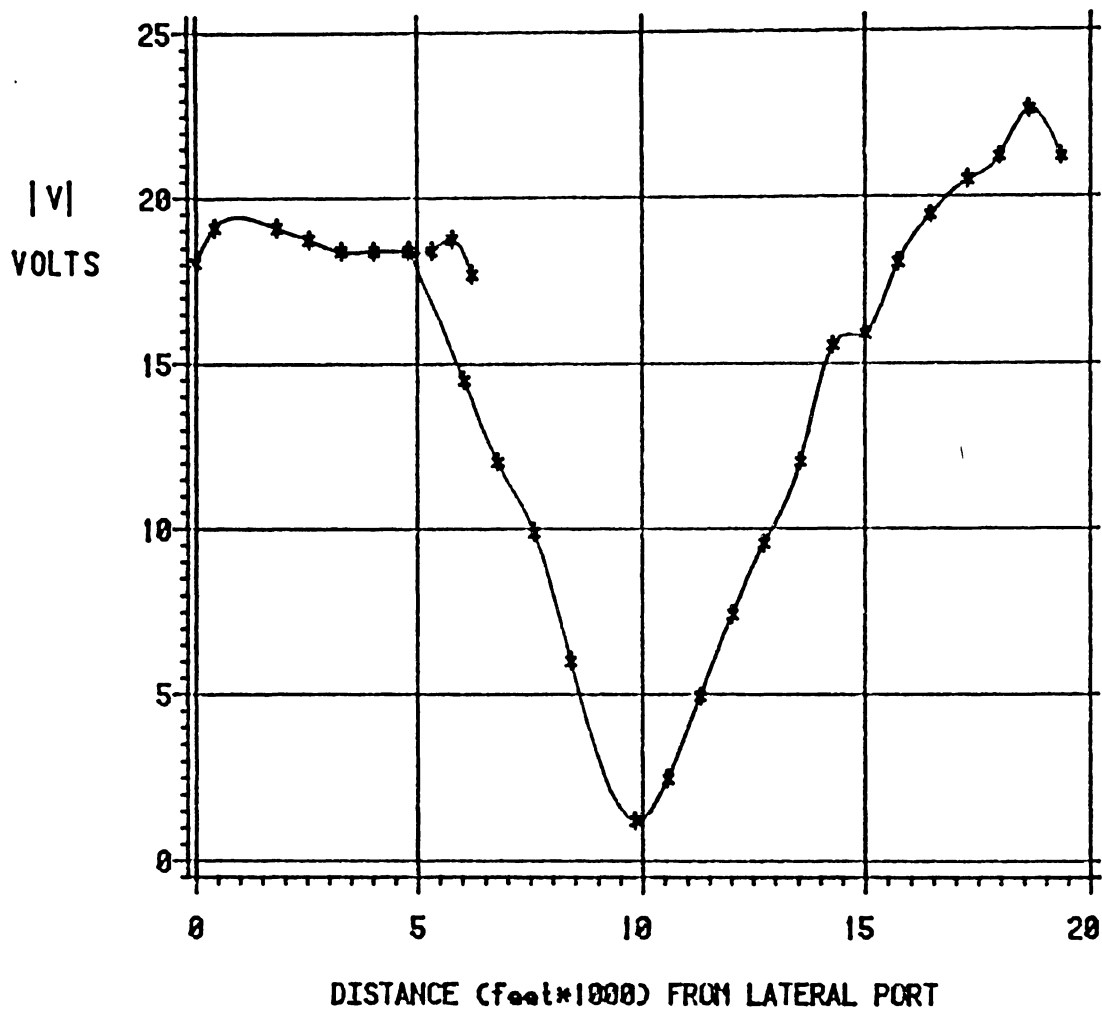


FIGURE 4.4.1 Measured network response for source at port LATERAL.  
Distances from source.

100 ohm source impedance.

# NETWORK TRANSIMPEDANCE

measured and predicted

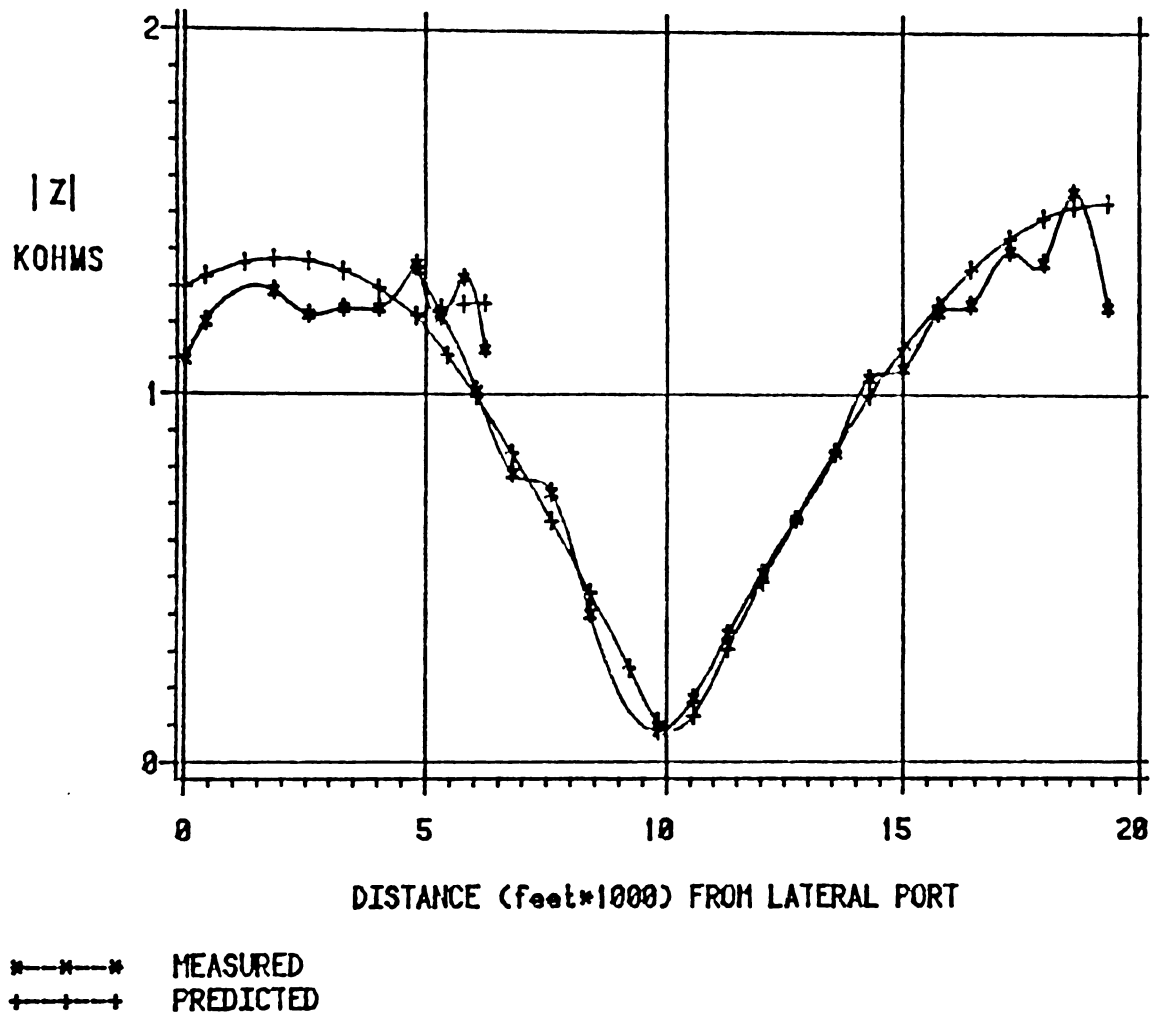


FIGURE 4.4.2 Measured and predicted network transimpedance for source at port LATERAL, distances from source.

100 ohm source impedance.

to the MAIN port. The results are plotted in Figures 4.4.3-4.4.4.

In Figure 4.4.5, the measured values of network transimpedance for each of the three cases of source locations are plotted against each other, as a function of distance from the HOST port. Where necessary, the origin (source) was translated to yield a common coordinate system.

Several observations can be made by examining Figure 4.4.5. First, the magnitude of the network transimpedance varies with the location of the source. For example, the network response to a given source current from the LATERAL port will be greater everywhere than the response due to the same current injected into the network from the MAIN port.

More significant, notice the shape of the function is dependent on the source location. In particular, the point in the network at which the response is at an absolute minima when the source was at the HOST port is not the same point at which the response is minimum when the source is at the MAIN port. In general, points of absolute and relative extrema, regions where the function increases or decreases, etc. do not all coincide.

This one significant example thus shows that the SNR throughout a network is not necessarily independent of position, when there is one predominant source of in-band noise.

Another set of measurements was conducted to demonstrate the distribution of noise voltage on the network when several major contributing noise sources are present. For these measurements, current was simultaneously injected into the network at all three ports identified in Figure 3.1.1. The three sources of current were derived from a single source by using the test set-up shown in Figure 4.4.6.

# NETWORK RESPONSE

source at MAIN

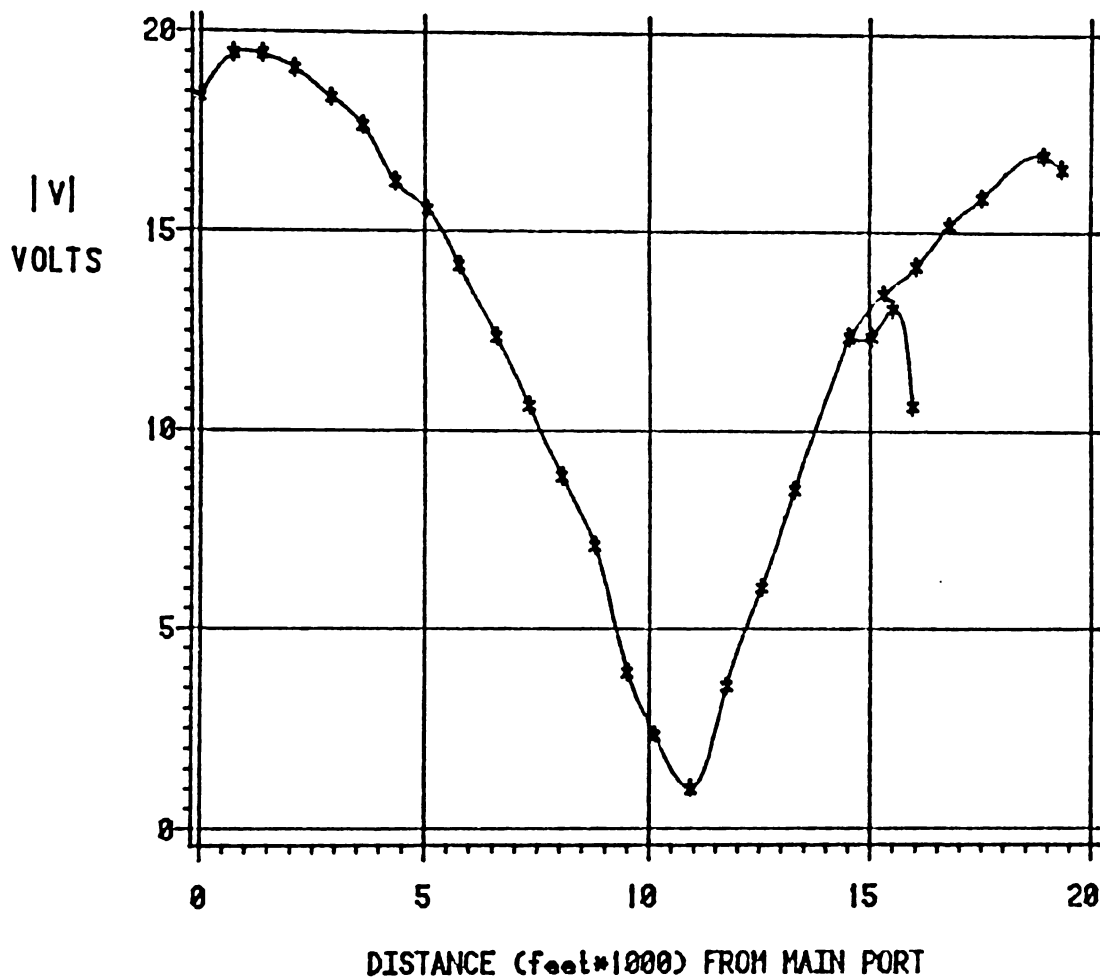


FIGURE 4.4.3 Measured network response for source at port MAIN, distances from source.

100 ohm source impedance.

# NETWORK TRANSIMPEDANCE

measured and predicted

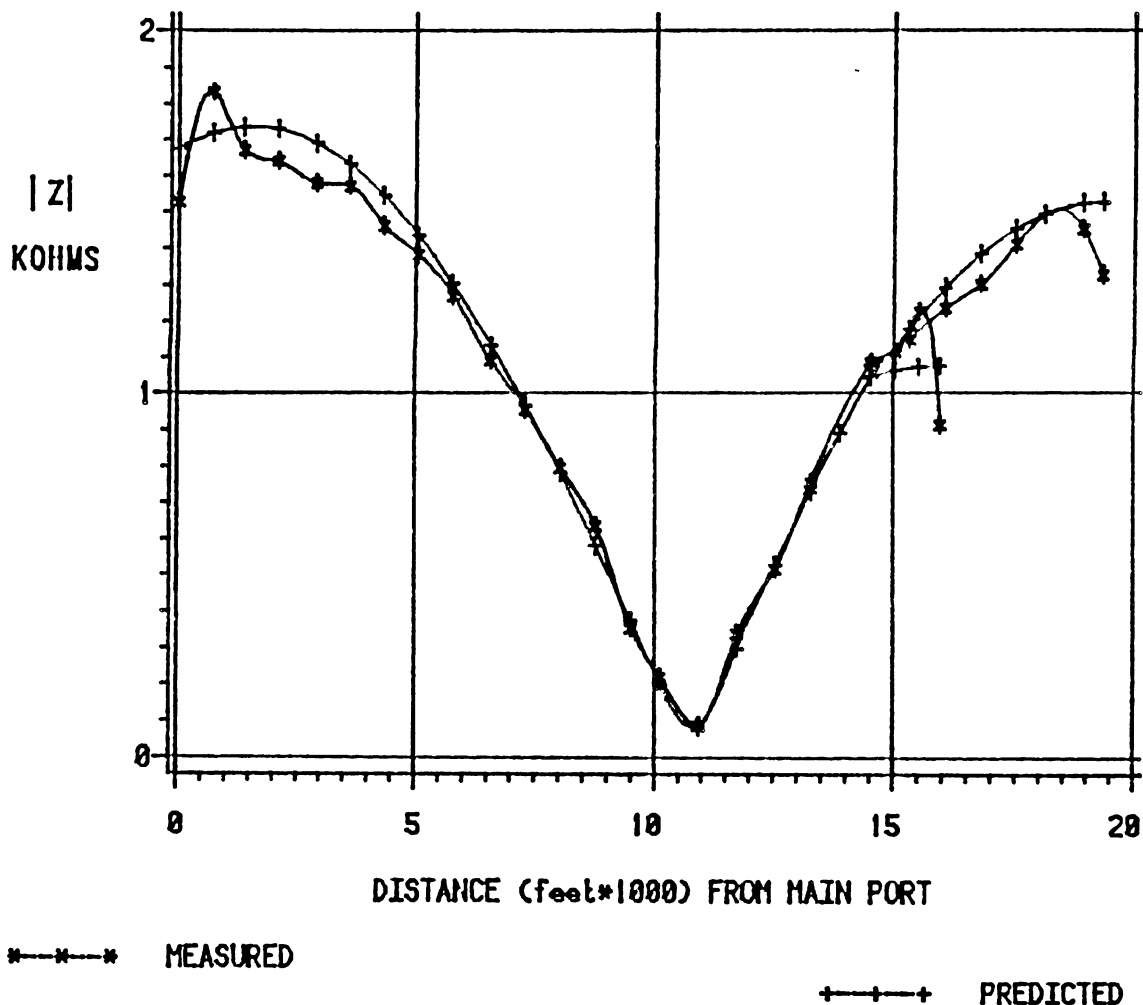


FIGURE 4.4.4 Measured and predicted network transimpedance for source at port MAIN, distances from source.

100 ohm source impedance.

# NETWORK TRANSIMPEDANCE

variable source location

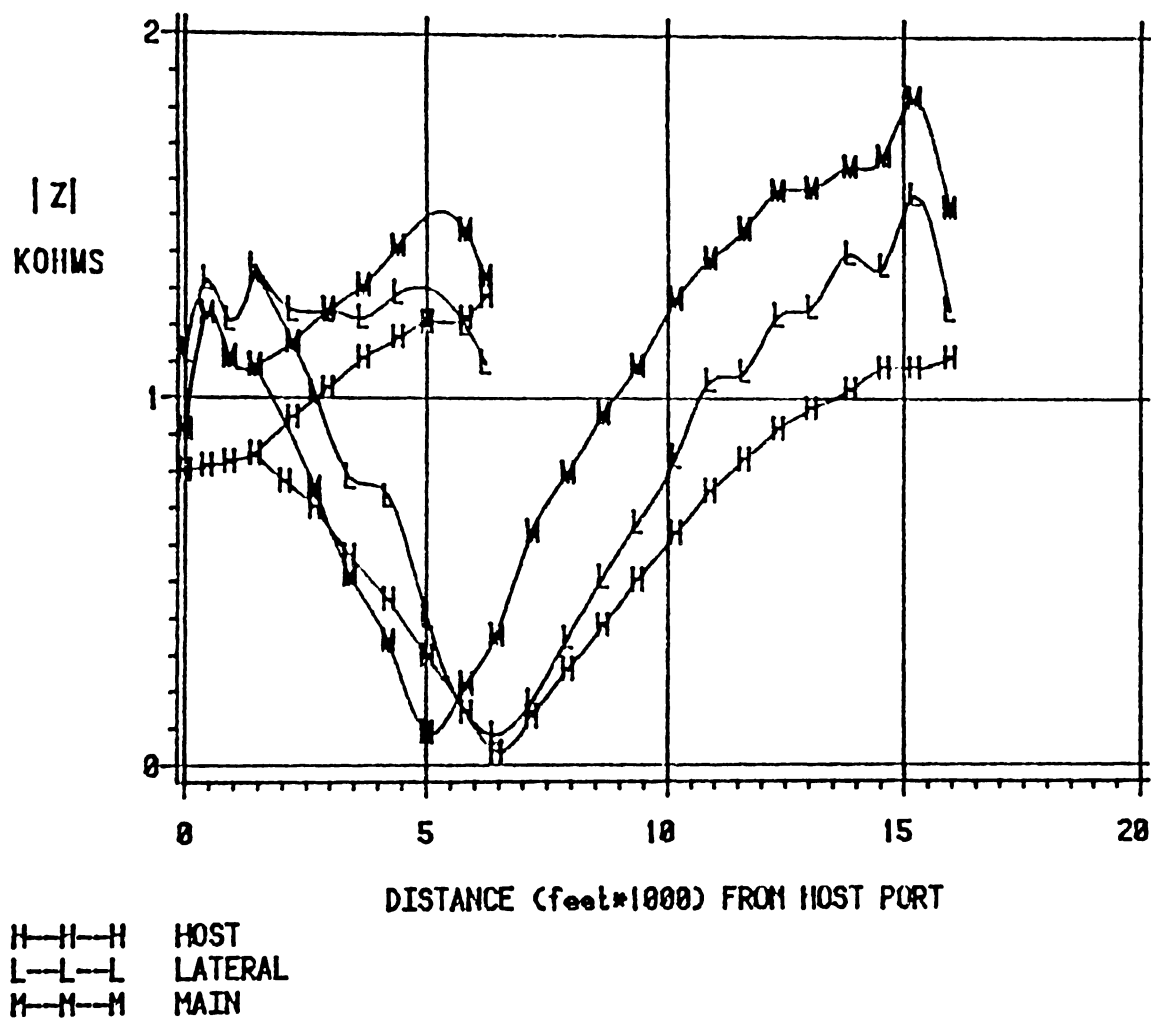


FIGURE 4.4.5 Measured network transimpedance for three source locations. 100 ohm source impedance.

Plotted as a function of network distance from HOST port.



The objective of this test is to measure the response of an unloaded network when excited at several different locations. To do this, it is necessary that the source impedances do not significantly load the line. This explains the choice of the 10 Kohm series impedances connecting each port to the single amplifier. This yields a reflection coefficient of approximately

$$p = \frac{10000 - 470}{10000 + 470} = 0.91$$

Therefore, only about one-tenth of the voltage from one source that would otherwise be reflected from an open-circuit is absorbed by the impedance of each of the other sources. This should approximate an open-circuit.

Incidentally, the same test could be performed by driving current into each port separately, and measuring the network response. Then, the composite response with each port being excited simultaneously could be calculated using superposition. However, since the network response is actually a complex vector, the individual responses cannot be added algebraically. This implies the phase of each of the responses must be known, which is difficult to measure.

In this test, the magnitude of each of the currents entering the ports were measured, along with the phase of each (using the HOST port as a reference). The network response was again measured, using the procedure outlined in Section 4.2. The results of the measurements are plotted in Figure 4.4.7. In this case, only the network response is

## NETWORK RESPONSE

network sourced from three ports

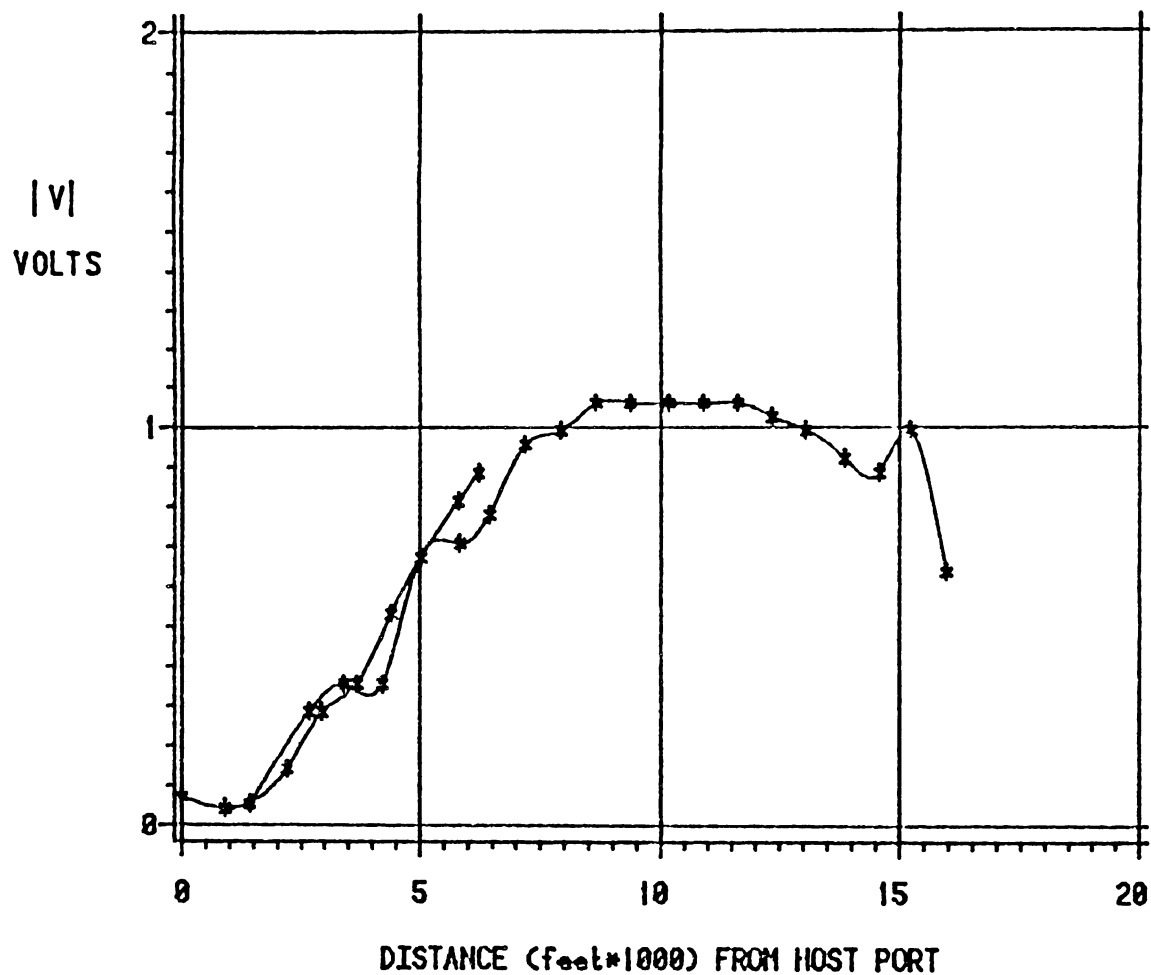


FIGURE 4.4.7 Measured network response with current sourced into three ports.

Plotted as a function of network distance from HOST port.

plotted, since the transimpedance is actually a function of the three sources.

Comparing the simulated noise profile of Figure 4.4.7 to the signal profile of Figure 4.2.4, it appears the the two bear little relation to each other. Regions of increasing and decreasing signal and noise as a function of network distance do not coincide. Similarly, locations peak and minimum signal do not coincide with the same extremes of the noise. Consequently, it is expected the signal-to-noise ratio of inbound communications (i.e., from the substation unit to the remote units) will vary widely at different locations, as the signal and noise have distinctly different profiles.

Notice this analysis does not apply to outbound communications (i.e., from the remote units to the substation unit). In this case, there is a single value of noise at the substation unit for given noise sources, their location, substation receiver input impedance, etc. The signal-to-noise ratio at the substation receiver depends only on the variations in the transimpedance to each remote unit (assuming equal output of these units).

## 5. CONCLUSIONS

The following conclusions regarding the behavior of signals and noise in branched single-phase distribution networks were reached as a result of this work:

- i.) The typical single-phase distribution network exhibits a symmetry with respect to the mutual impedances (transfer impedances) between pairs of ports into the network. This appears to be true regardless of the complexity of the network, and in the presence of standing waves. This result can be used to reduce the computation required to evaluate the performance of bi-directional systems.
- ii.) The network function (e.g. transimpedance) is not affected by the source. Therefore, "weak" spots in the communication signal occurring at points of low line impedance cannot be repositioned by changes at the signal source, for single-frequency (carrier) systems.
- iii.) Prediction of the network response, based on characteristics of the system elements previously developed, can be very sensitive to parameters of the network. In some networks, the error expected in the predicted values can be significant. Empirical data collected on several different test network configurations were in good agreement with prediction following "calibration" of the model.

- iv) Artificially loading the network by terminating long ( $>$  one-quarter wavelength) line sections with the line characteristic impedance, is effective in eliminating nulls in the network response. However, loading reduces the mean value of the transimpedance throughout the network, thereby ~~de-~~<sup>decreasing</sup> ~~grading the overall performance of the system.~~ <sup>This average signal strength in the system</sup>
- v.) The response of the network varies with the location of the source. Thus the DLC signal-to-noise ratio may vary with location in the network, even when a single source of noise is predominant.

## REFERENCES

- [CLI] Clinard, K. N., "Utility experience and desires for distribution power line carrier communications" IEEE Global Telecommunications Conference, Nov 28- Dec 1, 1983 487-491
- [CRE] Creamer, W. J. Communication Networks and Lines, Harper and Bros., New York, 1947.
- [DAV] Davis, T. W. and Palmer, R. W. Computer-aided Analysis of Electrical Networks. Charles E. Merrill, Columbus, OH, 1973
- [HEM] Hemminger, R. C. "The Effect of Distribution Transformers on Carrier Signal Propagation at Power line Carrier Frequencies", technical report, CCSP-TR-85/9, of the Center for Communications and Signal Processing, Box 7914, Raleigh, NC 27695-7914.
- [ONE] O'Neal, J. B. Jr. "Overview of Power Distribution Line Carrier Communications Systems" IEEE Global Telecommunications Conference, Nov 28- Dec 1, 1983 464-467
- [PAR] Paris, D. T. and Hurd, K. F. "Basic Electromagnetic Theory" McGraw-Hill, New York, NY, 1969.
- [SHU] Shuey, K. C. "Distribution Transformers at Power-Line Carrier Frequencies" IEEE Global Telecommunication conference, Nov 28- Dec 1, 1983 483-486
- [VAN] Van Valkenburg, M. E. "Network Analysis" Prentice-Hall, Englewood Cliffs, NJ 1974.
- [VIN] Vines, R. J. "The Characterization of Residential Impedances and Noise Sources for Power Line Carrier Communications", Master's Thesis, North Carolina State University, Raleigh, NC, 1983